Quaternary Research (2023), **111**, 1–20
doi:10.1017/qua.2022.33

Research Article

A multimethod approach to the genesis of Menga, a World Heritage megalith

Leonardo García Sanjuán[a]*, Alicia Medialdea[b], Verónica Balsera Nieto[c], Constantin Athanassas[d], Alistair Pike[e], Christopher D. Standish[e], Maria Isabel Dias[f,g], Ana Luisa Rodrigues[f], José Luis Clavero Toledo[h], David W. Wheatley[e] and Marta Cintas-Peña[a]

[a]Department of Prehistory and Archaeology, Universidad de Sevilla, María de Padilla s/n, 41004 Seville, Spain; [b]Centro Nacional de Investigación sobre la Evolución Humana (CENIEH), c/Paseo Sierra de Atapuerca 3, 09002 Burgos, Spain; [c]Ministerio de Derechos Sociales y Agenda 2030, c/Calle Ortega y Gasset 71, 28006 Madrid, Spain; [d]Department of Geological Sciences, School of Mining and Metallurgical Engineering, National Technical University of Athens (NTUA), Zografos, 15780 Athens, Greece; [e]Department of Archaeology, Southampton University, Faculty of Humanities, University Road, Southampton SO17 1BJ, United Kingdom; [f]Centro de Ciências e Tecnologias Nucleares (C2TN), Instituto Superior Técnico, Universidade de Lisboa, E.N. 10(km 139,7), 2695-066 Bobadela, Portugal; [g]Departamento de Engenharia e Ciências Nucleares (DECN), Instituto Superior Técnico, Universidade de Lisboa, E.N. 10(km 139,7), 2695-066 Bobadela, Portugal and [h]Sociedad Excursionista de Málaga, República Argentina, 9, 29016 Málaga, Spain

Abstract

The scientific study of Neolithic monuments holds fundamental keys to the analysis of early social complexity. This is often impeded by the challenges involved in understanding their temporality and, particularly, their initial construction dates. This problem is most severe in monuments that were not predominantly used for burial and went on to have long biographies in which activity in later periods obliterated the material record of the earliest phases. That was certainly the case of the Menga dolmen, part of the Antequera World Heritage site (Málaga, Spain), and one of the most remarkable megaliths in Europe, for which, after nearly 200 years of explorations and research, no firm chronology existed. The research presented in this paper shows how this problem was tackled through a multimethod, scientific, and geoarchaeological approach. The analysis of 29 fresh numerical ages, including radiocarbon determinations as well as optically stimulated luminescence, thermoluminescence, and uranium-thorium dates, led to the successful establishment of Menga's construction date and the subsequent contextualization of the monument within the social and cultural background it arose in. Placing the dolmen in the context of its time of "birth" introduces entirely new possibilities for its interpretation, both in terms of local and supralocal social and cultural processes.

Keywords: Neolithic, Megaliths, Radiocarbon, Bayesian modeling, Optically stimulated luminescence, Thermoluminescence, Uranium-thorium series

(Received 21 January 2022; accepted 16 June 2022)

INTRODUCTION

Megalithic monuments built during the Neolithic period hold fundamental keys to understanding the processes driving early social complexity (for seminal discussions, see Renfrew, 1973; Chapman, 1981, 1990; Sherratt, 1990; for recent overviews, see Meller et al., 2018; Müller et al., 2019; Laporte and Cousseau, 2020). However, methodological challenges remain that make that understanding quite difficult. The first and foremost challenge is the establishment of the monuments' temporality. While burial activity at Neolithic monuments is relatively easy to verify through the radiocarbon dating of human bone, establishing the age of their construction remains an outstanding challenge that has hampered prehistoric archaeology for decades. This problem is particularly pressing for megaliths that were not predominantly used for burial and is further compounded by the fact that, almost invariably, the most important constructions experienced activity well beyond the Neolithic period, into the Bronze Age and Iron Age, and even during historical periods, which often obliterated the evidence of early activity in and around them.

In this paper, an innovative multimethod approach is used to tackle this issue, revealing the age of construction and associated social and cultural context of one of Europe's most fascinating megalithic monuments: the Menga dolmen. Menga is part of the Antequera megalithic site (Málaga, Spain), one of the very few European megalithic complexes included in the UNESCO World Heritage Site List (Fig. 1). Antequera houses four major megaliths and two "natural" monuments closely associated with them. The four megaliths include Menga, which attained great fame throughout the nineteenth century (Sánchez-Cuenca, 2011) following the first explorations in the 1840s (Mitjana y

*Corresponding author at: Department of Prehistory and Archaeology, Universidad de Sevilla, María de Padilla s/n, 41004 Seville, Spain. E-mail address: lgarcia@us.es (L. García Sanjuán).

Cite this article: García Sanjuán L *et al* (2023). A multimethod approach to the genesis of Menga, a World Heritage megalith. *Quaternary Research* **111**, 1–20. https://doi.org/10.1017/qua.2022.33

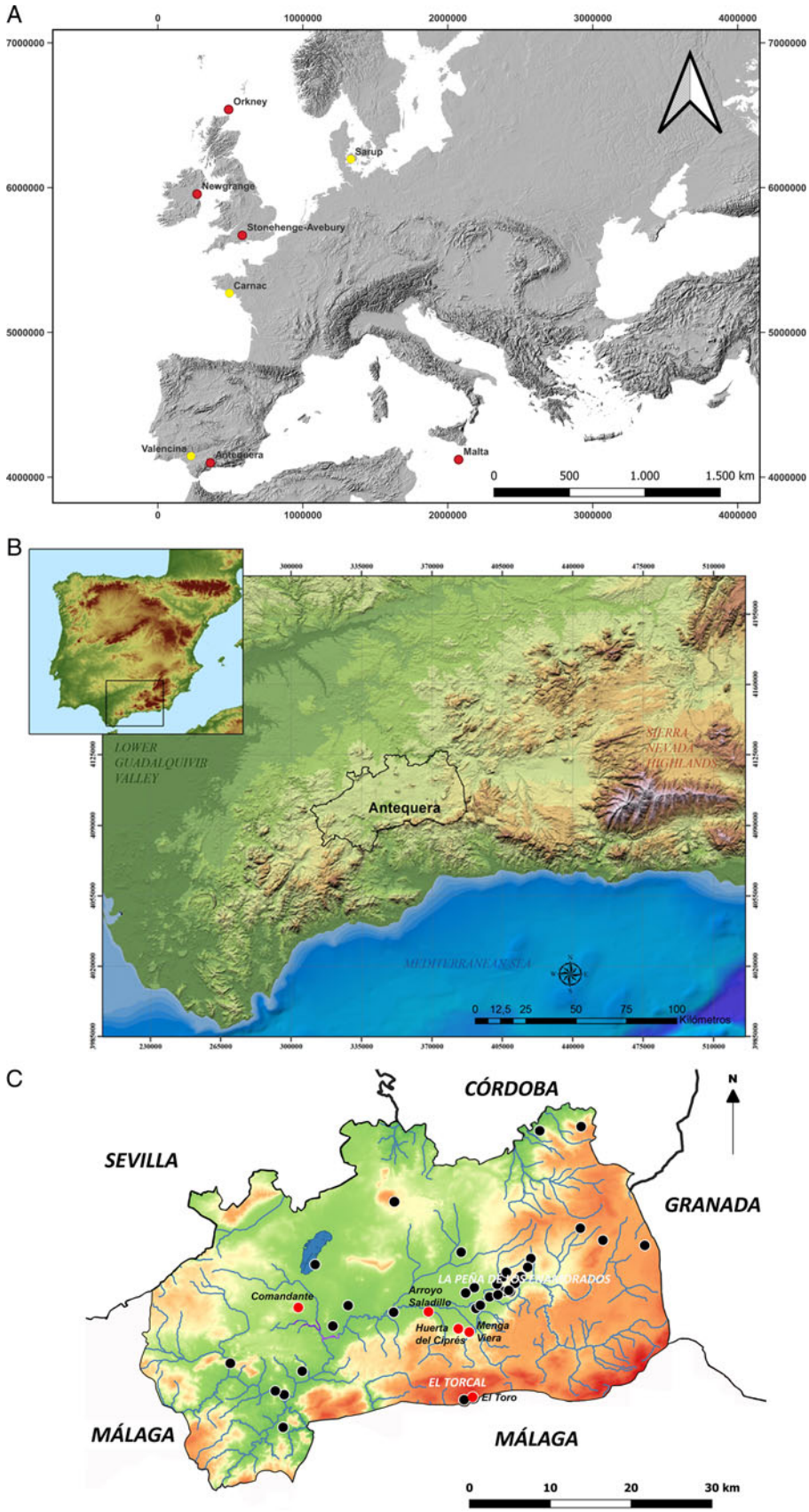

Figure 1. (A) Major earthen and megalithic monuments in fourth and third millennium western Europe (UNESCO World Heritage List in red; all others in yellow); (B) location of the Antequera region within the Iberian Peninsula; (C) distribution map of Neolithic sites in the lands of Antequera region (main sites discussed in the text in red; all others in black).

https://doi.org/10.1017/qua.2022.33 Published online by Cambridge University Press

Figure 2. Menga: (A) general view of the mound and entrance form the northeast (photograph: LGS); (B) plan showing the numbering of stones (design: Coronada Mora Molina, Universidad de Sevilla); (C) interior view from the back of the chamber (photograph: Miguel Ángel Blanco de la Rubia); (D) interior view from the back of the chamber with water well and Pillar 3 in the foreground (photograph: Coronada Mora Molina, Universidad de Sevilla).

Ardison, 1847); the Viera dolmen, discovered in 1903 barely 50 m southwest of Menga; El Romeral tholos, discovered in 1904 some 6 km east of Menga and Viera; and the Piedras Blancas megalithic structure, discovered as recently as 2020, as part of the research program this paper stems from. The two natural monuments include El Torcal, a karstic formation located 11 km south of the megaliths, and home to El Toro Cave, occupied since the Early Neolithic (ca. 5400 BCE); and La Peña de los Enamorados, a limestone massif rising 800 m above sea level and presiding over the skyline of the Antequera plain.

Menga is a remarkable monument. Located on a hilltop (Fig. 2A), its inner space, measuring 24.9 m in length, with a maximum width of 5.7 m and a height rising from 2.5 m at the entrance to 3.45 m at the back of the chamber, is enclosed by 12 uprights on each side plus a massive backstone and covered by five capstones (Fig. 2B). The feat involved in the construction of this dolmen is best reflected by the magnitude of the colossal stones used to build it, with a combined estimated weight of well over 800 tons. Capstone C-5, at the back of the chamber (Fig. 2C), is the largest of all, with an estimated weight of 170 tons, which makes it the largest stone ever moved as part of the megalithic phenomenon in Iberia, and one of the largest in Europe. By comparison, the sarsen stones used in Stonehenge (UK), which were added in ca. 2500 BCE to the already existing ditched enclosure, weigh an average of 25 tons, with the largest of them, the so-called Heel Stone, weighting ca. 30 tons (Parker Pearson, 2012). Another important element in Menga's architectural design is the presence of three large pillars aligned with the chamber's longitudinal axis, below the joints of the four inner capstones (Fig. 2C and D). The mound covering the construction presents a diameter of 48.3 m in the northeast to southwest axis and 44 m in the northwest to southeast axis, covering a surface of ca. 2.730 m^2. This stout tumulus has provided protection and stability to the construction for almost 6000 years.

Three other elements add to the uniqueness of Menga. The first of them is the water well located at the back of the chamber (Fig. 2D). With 19.4 m of depth and 1.5 m of width (slightly narrower at the bottom), this well provides access to fresh water, which makes it a unique hydraulic feature within the context of the megalithic phenomenon worldwide. Indeed, Menga's long biography runs in parallel with the complex history of local water resources (García Sanjuán et al., 2021). The second element to be noted is the landscape aspect of the dolmen. Unlike most Iberian megaliths, which face sunrise between the summer and winter solstices (Hoskin, 2001), Menga's axis of symmetry points to 45°, about 10° north of the summer solstice. Thus, Menga faces the northern sector of La Peña de los Enamorados mountain, where at the time of its construction intense activity was already taking place around the Matacabras sanctuary, which includes rock art paintings of the "schematic" style (García Sanjuán et al., 2015; Rogerio-Candelera et al., 2018). The megalithic monument recently discovered at the foot of Matacabras adds to the significance of La Peña's northern sector. However, it is important to note that, although Menga's orientation prioritized a land "target" and was not made to fall between the range of the solstices, as is customary in Iberia, its design also sought to integrate

https://doi.org/10.1017/qua.2022.33 Published online by Cambridge University Press

architecture and sunlight (Lozano-Rodríguez et al., 2014), thus seeking a sunlight effect in a manner best reflected in Newgrange (Ireland) (Patrick, 1974). Third, Menga is quite remarkable because it appears to have been in constant use since its original construction, never falling into oblivion—the inevitable fate awaiting most prehistoric megaliths at one point or another. The stratigraphic deposits and material culture associated with the dolmen reveal clear evidence of its use during the Copper Age, Bronze Age, Iron Age, antiquity, Middle Ages, and modern history (García Sanjuán and Lozano Rodríguez, 2016).

Despite all this, the construction date of Menga and its temporality as a monument have essentially been a mystery until now. The seriousness of this problem is best reflected in the fact that, as late as 2016, not a single radiocarbon date had been published for it. This is all the more striking in light of the set of characteristics that makes it such an exceptional monument (the true "flagship" of the Antequera site, itself only matched by Altamira and Atapuerca as the main "icons" of Spanish Prehistory) and the almost 200 years elapsed since the first explorations, a period that has witnessed a substantial number of archaeological interventions. Paradoxically, although a true quantum leap has been achieved within the last decade, progressing from 0 to 61 radiocarbon dates for Menga, those dates published up to now provide mostly historical ages, thus reflecting activity at the monument and its surroundings in antiquity, the Middle Ages, and modern history (García Sanjuán et al., 2018a). Such a data set did not provide the kind of precise information needed to date Menga's construction, which occurred in the Neolithic. Needless to say, this in turn prevented any in-depth understanding of the social and cultural circumstances that made such a remarkable monument possible.

Using an innovative multimethod approach, we have obtained 29 new numerical ages over the last 7 years, including 12 radiocarbon, 11 optically stimulated luminescence (OSL), and 6 uranium-thorium series (U-Th) dates. They are presented in this paper for the first time. As will be shown later, this data set provides the basis to build a fresh high-resolution multimethod chronometric model of Menga's construction, which in turn allows for an entirely new analysis of its genesis as a monument. For the first time in almost 200 years of research, a sound understanding of the sociocultural background surrounding the construction of Menga, both locally (including the occupancy, frequentation, and ritual use of other sites known in the region) and regionally (the wider arena of changes occurring in the Late Neolithic period) is possible.

SAMPLING AND METHODS

Radiocarbon Dating

In total, 12 samples of charred material and animal bone from Menga (9) and El Toro (3) were submitted for radiocarbon dating to the Centro Nacional de Aceleradores (Seville, Spain) and Beta Analytic. They were pretreated, graphitized, and measured as described by Santos Arévalo et al. (2009). The reported $\delta^{13}C$ values were measured by accelerator mass spectrometry. All calibrations were made with OxCal 4.4 (Bronk Ramsey, 1995) based on the IntCal20 Northern Hemisphere radiocarbon age calibration curve (Reimer et al. 2020).

In the case of Menga, all nine new radiocarbon determinations (Table 1), were drawn from samples collected from Trench 1 of the excavation undertaken by the University of Granada between September 2005 and March 2006. Trench 1 (Fig. 3), 27.4 m long and 3 m wide, was located on the northwestern sector of the dolmen's mound, between its summit and the track opened in the 1940s to facilitate the access of motor vehicles all the way to the dolmen's entrance, which broke a large section of the mound. Trench 1 allowed documentation of the stratigraphy of the mound, which was composed basically of two main layers. The deepest, 1.5 m thick and composed of very dark soil, yielded large amounts of organic material and substantial quantities of hand-thrown pottery and knapped flint. Eight radiocarbon dates were obtained from samples of this layer, which provided in all cases Late Neolithic ages (fourth millennium BCE) as will be described in the "Results." This layer integrates sediments collected from the very same hill where Menga was built and essentially reflects the intense activity the hill witnessed before and during the construction of the monument. Therefore, the radiocarbon determinations obtained from this layer provide *post quem* ages for the erection of the dolmen. The upper layer of the mound, some 3 m in depth, was made with alternating layers of carefully locked medium-size sandstone slabs and rammed clay. Undoubtedly, this robust device, enveloping the megalithic chamber, has played a major part in its preservation, protecting it from weathering and geological events. One radiocarbon determination (Beta-526347) comes from a sample taken from the westernmost end of Trench 1 and represents a different event—perhaps the expansion of the mound sometime after the original construction of the dolmen (Mora Molina, 2018, p. 737). For this reason, this particular determination has been used as an *ante quem* age with respect to the primary construction of Menga. Five of these nine dates were obtained from samples of charred material, while the other four are from samples of nonarticulated animal bones (Table 1). All these dates provide very consistent ages between ca. 3900 and 3400 BCE, with the exception of Beta-526347, which provides a slightly later age, which is in keeping with its stratigraphic position.

The nine new Menga ^{14}C dates were combined with three previously published ones, which were obtained from samples of charred material extracted from a pit (Structure 9) located at the atrium and from the base of the mound (García Sanjuán and Lozano Rodríguez, 2016, p. 5). As mentioned earlier, several other radiocarbon dates have been published for Menga and its surroundings, all of which provided historical ages and therefore are not relevant to establish its construction date.[1]

In the case of El Toro, a cave located at El Torcal karst that holds important keys to understanding the cultural background to early monumentality in the Antequera region, three samples of charred material were obtained for radiocarbon dating. Excavated in the late 1980s and early 1990s (a full description is available in Martín Socas et al., 2004), El Toro is a good example of an Early Neolithic habitat, resulting from the spread of the first farming communities along the Mediterranean coasts of Iberia between ca. 5600 and 5400 BCE. As shown by a robust series of 29 radiocarbon determinations (Egüez et al., 2016) (Table 2), this cave was used as a habitation and as an animal pen, probably also witnessing some ritual activity (Egüez et al., 2016; Santana et al., 2019), since the second half of the sixth millennium BCE and throughout the entire fifth millennium BCE. In

[1]These include 8 determinations obtained from various Roman era tombs and structures located around the dolmen, which revealed significant activity in antiquity (Aranda Jiménez et al., 2015, p. 274); 16 from the infill of the water well, all of which provided modern ages between the fifteenth and eighteenth centuries CE (García Sanjuán et al., 2016); and 34 from three sites located in the Antequera plain: Arroyo Saladillo (20 dates), Huerta del Ciprés (13), and El Comandante (1) (García Sanjuán et al., 2020).

https://doi.org/10.1017/qua.2022.33 Published online by Cambridge University Press

Table 1. New radiocarbon determinations of Neolithic age for Menga.

Lab code	Sample code[a]	Sample material	Context[b]	Date BP	Date 2σ cal BCE	$\delta^{13}C$ ‰	Reference	Implication for construction date
CNA-5040	A/DJ 14541-91-FIS	Charred material (*Phillyrea* sp.)	Trench 1 (mound)	5050 ± 30	3952–3776	−15.51	This paper	*Post quem* (before construction)
CNA-5039	A/DJ 14541-90-QIC	Charred material (*Quercus ilex coccifera*)	Trench 1 (mound)	5000 ± 30	3938–3701	−19.82	This paper	*Post quem* (before construction)
Ua-24582	Structure 9, Layer 3, Sample 1	Charred material (indetermined)	Structure 9 (pit), UE 3 (Atrium) (X_4)	4935 ± 40	3790–3640	−27.1	García Sanjuán and Lozano Rodríguez, 2016	Could be before, simultaneous with, or after construction
Ua-24583	Structure 9, Layer 3, Sample 2	Charred material (indetermined)	Structure 9 (pit), UE 3 (Atrium) (X_4)	4865 ± 40	3760–3530	−28.5	García Sanjuán and Lozano Rodríguez, 2016	Could be before, simultaneous with, or after construction
CNA-5041	A/DJ 14541-95-QIC	Charred material (*Quercus ilex coccifera*)	Structure 9 (pit), UE 1 (Atrium) (X_4)	4880 ± 30	3707–3636	−23.45	This paper	Could be before, simultaneous with, or after construction
Beta-526345	A/DJ 14541-203-3	Bone (deer, mandible)	Trench 1, Sector D, Layer 2 (mound) (X_1)	4780 ± 30	3650–3510	−19.40	This paper	*Post quem* (before construction)
Beta-526346	A/DJ 14541-73-1	Bone (cow, metacarpal)	Trench 1, Sector D, Layer 1 (mound) (X_1)	4780 ± 30	3650–3510	−19.30	This paper	*Post quem* (before construction)
Ua-36216	NA	Charred material (indetermined)	Mound (lower infill)	4760 ± 30	3639–3384	−24.5	García Sanjuán and Lozano Rodríguez, 2016	*Post quem* (before construction)
CNA-5038	A/DJ 14541-90-ARU	Charred material (*Arbustus unedo*)	Trench 1 (mound)	4760 ± 30	3639–3384	−25.67	This paper	*Post quem* (before construction)
Beta-526344	A/DJ 14541-203-2	Bone (ovicaprine, upper tooth)	Trench 1, Sector D, Layer 2 (mound) (X_1)	4750 ± 30	3640–3380	−18.50	This paper	*Post quem* (before construction)
Beta-526337	A/DJ 14541-142-OLE	Charred material (*Olea europea*)	Trench 2, Structure 31 (X_3)	4750 ± 30	3640–3380	−25.60	This paper	Could be before, simultaneous with, or after construction
Beta-526347	A/DJ 14541-73-2	Bone (cow, first phalanx)	Trench 1, Sector E, Layer 1 (mound) (X_2)	4580 ± 30	3500–3110	−19.40	This paper	*Ante quem* (enlargement of mound after construction)

[a]NA, not available.
[b]X_1, X_2, X_3, and X_4 refer to the locations of the samples as shown in Fig. 3A (plan of Menga excavations).

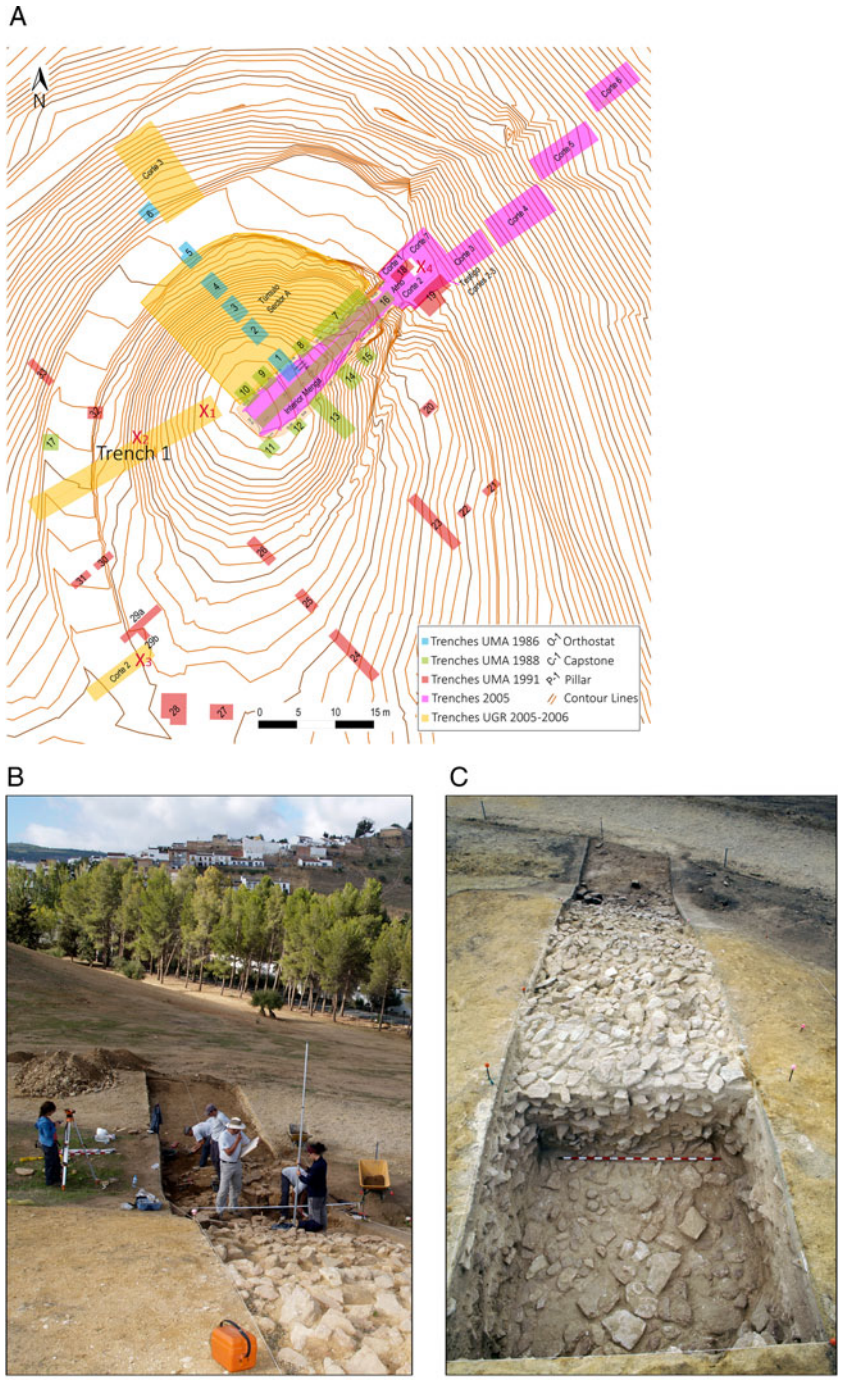

Figure 3. Menga: (A) location of Trench 1 of the 2005–2006 excavation in Menga with reference to other excavated areas of the dolmen (design: Coronada Mora Molina, Universidad de Sevilla); (B) general view of excavation activity in September 2005 at Trench 1, taken from the east (photograph: David García González, CSIC); (C) general view of Trench 1, revealing the construction system of Menga's mound, with alternating layers of medium-sized stone slabs and pressed clay (photograph: David García González, CSIC).

their conclusions, the excavators claimed that El Toro Cave was abandoned because of an earthquake that caused a dramatic change in its topographic conditions, including the lasting blockage of its main entrance and the collapse of a major slab from the roof (Martín Socas et al., 2004, p. 297). It is worth noting that Antequera is located in one of the most seismic areas of the Iberian Peninsula (Lario et al., 2010; Grützner et al., 2013). This slab, measuring about 12 m in length and 4 m in width, lies at the far end of the cave's main chamber (Fig. 4C and D). However, the chronology and possible causes of the fall of this slab, potentially relevant to understand the abandonment of the cave, were never established. The three newly dated samples provided ages that also fall within the Late Neolithic period (Table 3), as will be discussed later.

Bayesian chronological modeling was applied to the newly obtained dates for both Menga and El Toro, in combination with

https://doi.org/10.1017/qua.2022.33 Published online by Cambridge University Press

Table 2. Radiocarbon determinations for El Toro (after Egüez et al., 2016).

Phase	Ref. Lab.	BP	BCE (1 σ)	BCE (2 σ)
First phase of occupation	UGRA-194	6400 ± 280	5650–5000	5879–4721
	Beta-174305	6540 ± 110	5620–5370	5670–5290
	GrN-15443	6320 ± 70	5460–5140	5480–5070
	Beta-174308	6160 ± 40	5210–5000	5260–4950
	Beta-341132	6150 ± 30	5210–5040	5210–5000
	GRN-15444	6030 ± 70	5020–4800	5210–4720
	Beta-341131	6110 ± 30	5050–5000	5200–4950
	GRN-15440	5820 ± 90	4780–4550	4910–4450
	Gak-8059	5320 ± 230	4450–3800	4700–3600
Second phase of occupation	Gak-8060	5450 ± 120	4450–4050	4550–3950
	GRN-15445	5380 ± 45	4330–4050	4340–4040
	I-17552	4910 ± 190	3950–3510	4300–3100
	Beta-343182	5320 ± 30	4230–4050	4250–4040
	GRN-15436	5250 ± 60	4220–3970	4250–3950
	Beta-174306	5240 ± 70	4220–3960	4250–3820
	Beta-347631	5300 ± 30	4230–4050	4240–4000
	Beta-343180	5290 ± 30	4227–4046	4233–4002
	Beta-347633	5280 ± 30	4227–4043	4232–3996
	Beta-341130	5270 ± 30	4225–4000	4231–3990
	GrN-15437	5200 ± 60	4220–3950	4230–3800
	Beta-343179	5260 ± 30	4224–3993	4229–3985
	Beta-343181	5240 ± 30	4050–3990	4220–3970
	GRN-15439	5205 ± 40	4045–3960	4220–3940
	Beta-343183	5210 ± 30	4040–3970	4050–3960
	Beta-336259	5170 ± 30	4033–3959	4043–3947
Abandonment				
Sporadic frequentation	Beta-174307	4800 ± 80	3660–3380	3720–3360
	I-17553	4120 ± 120	2880–2500	3050–2300
	UGRA-189	3090 ± 130	1500–1130	1700–950
	GRN-15446	2880 ± 50	1190–940	1260–910

already existing ones whenever necessary. Bayesian modeling is based on the principles of Bayesian statistics (Lindley, 1985) and operates by combining calibrated radiocarbon dates with archaeological information using a formal statistical methodology (Buck et al., 1996; Bronk Ramsey, 2009). The resulting chronometric models are more robust and precise than those based exclusively on stratigraphic inferences or scientific dating alone. To produce Bayesian chronologies, alternative models must be created and explored to test different hypotheses (García Sanjuán et al., 2018b).

Thus, several Bayesian models were calculated, based on the following criteria of "chronometric hygiene": (1) multiphase models were calculated through the incorporation of sequential phases, assuming that time lapses may have existed between them; (2) modeled dates (all of them calibrated) were rounded to 5 years; (3) only radiocarbon determinations with standard deviations smaller than 100 were used; (4) results were calibrated to 1σ and 2σ; (5) for each range, medians (μ) were also estimated; and (6) a Bayesian model was considered statistically robust when its verisimilitude index was equal to or greater than 60 (A_{model}).

OSL dating

To obtain a more accurate date for Menga's construction, OSL was used to complement radiocarbon dating. Numerical dating by OSL considers the time elapsed since the last exposure of mineral grains (typically quartz or feldspar) to sunlight or heat (in the case of heated lithics or ceramics) and is equal to the dose received during burial over the rate the dose was delivered (dose rate). The (absorbed) dose (Gy) is obtained by dosimetry, that is, applying luminescence protocols that evaluate the natural dose against its laboratory equivalent (D_e), the laboratory radiation dose (accumulated energy) needed to induce "artificial" (OSL) signals

https://doi.org/10.1017/qua.2022.33 Published online by Cambridge University Press

Figure 4. El Toro: (A) general overview of El Torcal karstic formation (photograph: Coronada Mora Molina, Universidad de Sevilla); (B) general plan of the cave (after Martín Socas et al., 2004, p. 29, figure 3); (C) general view of the cave, with large fallen roof slab in the background, next to person standing (photograph: DWW): (D) Detail of the sample extraction for radiocarbon and OSL dating, underneath and above the fallen roof slab in June 2017 (photograph: AM).

equal to the natural signal (Aitken, 1985, 1999; Liritzis, 2011; Athanassas et al., 2015). The dose rate (D_r) represents the rate at which energy is delivered (Gy/ka) from the flux of nuclear radiation (alpha, beta, and gamma radiation) due to the decay of natural radioactive elements (U, Th, K, Rb) as well as from cosmic rays. D_r is evaluated by measuring the radioactivity of both the sample and its surrounding burial material through well-established analytical (chemical analyses) or gamma spectrometry methods. Dosimetric gamma spectrometry can be performed either in the laboratory or in the field (in situ gamma spectrometry) (Aitken, 1999; Burbidge et al., 2014). In any case, the cosmic-ray component should be modeled independently and added to the dose rate. The dose rate is corrected relative to water content and granulometry of the studied material (Odriozola et al., 2014; Rodrigues et al., 2019).

OSL is regarded as a good alternative to establish the temporality of major monuments when well-contextualized organic remains are scarce or unavailable (López-Romero, 2011; Rodrigues et al., 2019). This is exactly the situation at Menga, which suffers from a complete lack of Neolithic human bone and a dearth of animal bone associated with its construction phase and early use. In general, the application of OSL to the dating of megalithic monuments started very recently (Galli et al., 2020; Shewan et al., 2021; Parker Pearson et al., 2021; Kim et al., 2022). In Iberia, despite some earlier

Table 3. New radiocarbon determinations for collapse of El Toro cave roof slab.

Lab code	Sample code	Context	Date BP	Date 2σ cal BCE	$\delta^{13}C$ ‰	Implication for collapse of slab	Bibliographic Reference
Beta-429656	ETC-7	Unidentified sediment material from above the large fallen roof slab	5080 ± 30	3969–3797	25.8	*Post quem* (after collapse of slab and abandonment of cave)	This paper
Beta-428897	ETC-6	Unidentified charred material from above the large fallen roof slab	5220 ± 30	4221–3964	−26.0	*Post quem* (after collapse of slab and abandonment of cave)	This paper
Beta-428896	ETC-5	Unidentified charred material from below the large fallen roof slab	5870 ± 30	4827–4687	−25.4	*Ante quem* (before collapse of slab and abandonment of cave)	This paper

https://doi.org/10.1017/qua.2022.33 Published online by Cambridge University Press

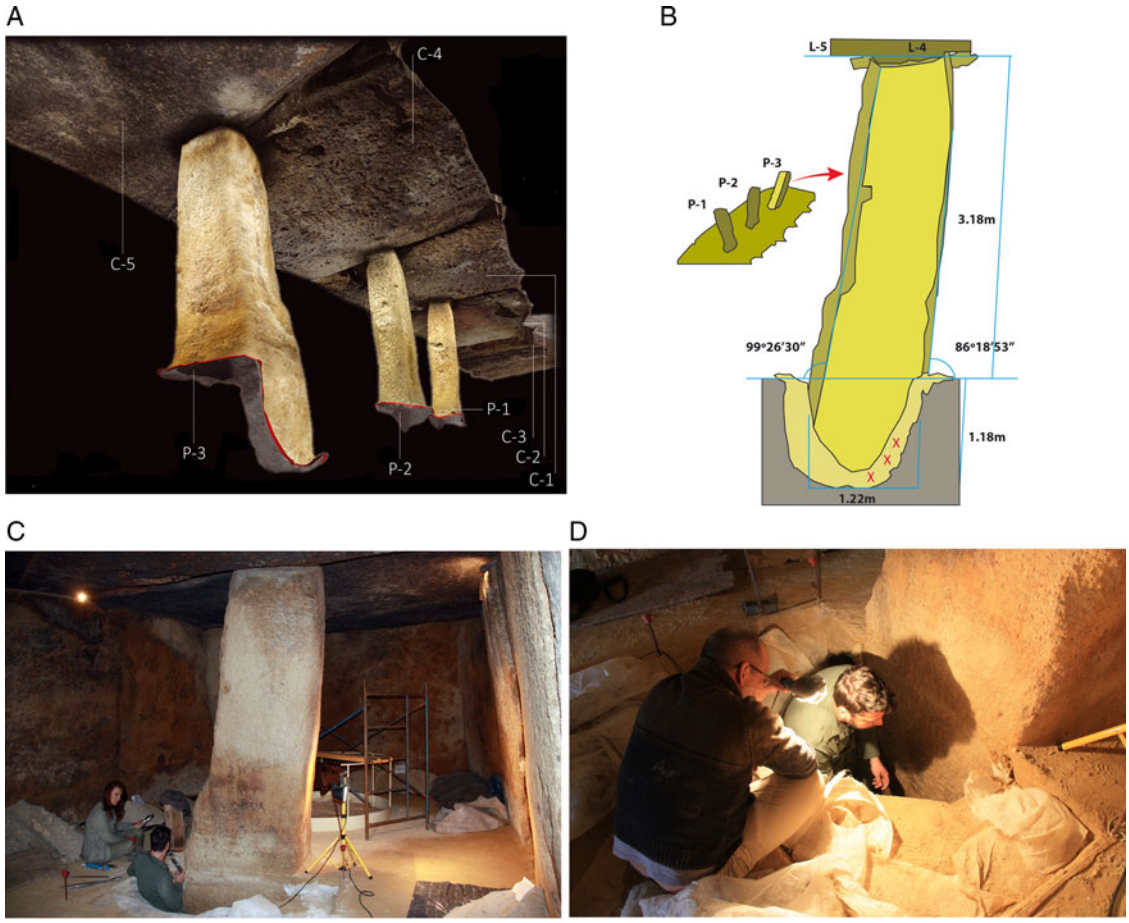

Figure 5. Menga: (A) location of Pillar 3 with regard to Capstones 4 and 5 based on the laser-scanning photogrammetry of the monument (design: LGS, after Baceiredo Rodríguez et al., 2014); (B) section of Pillar 3 (P-3) and socket (precise location each dated OSL samples is marked with a red *X*; design: José Antonio Lozano Rodríguez, CSIC); (C) general view of the excavation process inside the socket of Pillar 3 (photograph: LGS); (D) detail of the sample-extraction process inside the socket of Pillar 3 (photograph: Katerina Theodorakopoulou, University of Athens).

attempts (see Calado, 2003; López Romero, 2011; Athanassas et al., 2016, 2017), the use of OSL is still not widespread, and its full potential has not yet been realized.

OSL using the single-aliquot regenerative protocol (Murray and Wintle, 2000) was measured from a total of three samples collected in 2014 from the foundation sockets (and associated infills) of the uprights and pillars of the dolmen (Fig. 5C and D, Table 4). This assumed that a sufficient amount of grain of the sediment should have time and conditions for an adequate exposure to daylight during collection and transportation from its geological source and trickling into the socket at the time of construction. Therefore, good bleaching conditions are assumed, resetting the geological OSL signal before the construction of the monument. Sampling was based on the following reasoning. Pillar 3 does not stand perfectly vertically, but leans some 4° to the north (Fig. 5B). For this reason, its lower third leans to the northern side of the socket cut as its foundation to a depth of 1.18 m. Thus, although the inner areas of the dolmen, including the sockets of the uprights and pillars, have been extensively excavated since the nineteenth century, we anticipated that undisturbed fractions of the sediments of the infill used originally inside the socket of Pillar 3 would have remained within the narrow space between its northern side and the northern side of the socket. Indeed, infill sediment trapped between Pillar 3 and the socket's

Table 4. Optically stimulated luminescence (OSL) ages for Menga and El Toro.

Sample code	Sample material	Context	Dose rate (Gy/ka)	Equivalent dose (Gy)	Age (ka)	Date BP	Date BCE	Bibliographic reference
MENGA2Socket	Infill	Socket of Pillar 3	1.03 ± 0.03	6.0 ± 0.3	5.8 ± 0.3	5719 ± 304	3769 ± 201	This paper
MENGA1Infill	Infill	Socket of Pillar 3	0.95 ± 0.09	5.2 ± 0.4	5.5 ± 0.4	5467 ± 365	3517 ± 325	This paper
MENGA1Contact	Infill	Socket of Pillar 3	1.00 ± 0.03	5.5 ± 0. 8	5.5 ± 0.8	5493 ± 790	3543 ± 510	This paper
CET-OSL2	Soil	Above fallen roof slab	1.73 ± 0.09	8.3 ± 0.3	4.8 ± 0.3	4731 ± 282	2781 ± 166	This paper
CET-OSL3	Soil	Below fallen roof slab	1.45 ± 0.06	7.5 ± 0.2	5.1 ± 0.3	5063 ± 267	3113 ± 164	This paper

https://doi.org/10.1017/qua.2022.33 Published online by Cambridge University Press

northern face was retrieved at three locations (marked in Fig. 5B). This sediment was found to be more cohesive than the surrounding sediment (another evidence of its relatively older age) and allowed the insertion of thin aluminum tubes (Fig. 5D) to capture the samples undisturbed.

An earlier attempt at dating the infills from the sockets of Menga (Athanassas et al., 2016) was clouded by large uncertainties due to the infiltration of a considerable amount of unrest grains into the measured multigrain aliquots. The luminescence signal from single grains was then measured to increase the resolution and distinguish the population of grains most likely to be fully reset at the time of construction. This method provided a largely resolved distribution with a well-defined dominant peak from which the burial dose could be estimated by applying the internal–external uncertainty model (IEU; Thomsen et al., 2007).

At El Toro Cave, two samples of sediment accumulated below and above the fallen slab described earlier were collected for OSL dating. All four samples were retrieved from the southern third of the slab (their positions were only recorded photographically, as no detailed plan of this slab exists). The sample under the slab was not sealed, and therefore it could not be guaranteed that it was deposited before the collapse of the roof.

All OSL samples were collected so as to avoid exposure to daylight and were treated under controlled light conditions. OSL was measured on the quartz fraction of each sample based on multigrain aliquots, which have been shown to provide enough resolution to estimate the true burial dose and the corresponding age of flood deposits (Medialdea et al., 2014). Dose distribution of the sediment under the slab was normally distributed, and the central age model (Galbraith et al., 1999) was suitable for calculating the burial dose, whereas dose distribution of the sediment on top of the slab was largely scattered, so the IEU model (Thomsen et al., 2007) was considered more appropriate to estimate the burial dose in this case.

For the environmental dose rate estimation, *in situ* field gamma measurements were performed using a gamma spectrometer (HPI Rainbow MCA with a 3 inch x 3 inch NaI probe). Stripped counts in the windows 1380–1530 keV, 1690–1840 keV, and 2550–2760 keV (designed to obtain signals dominated by ^{40}K, ^{214}Bi, and ^{208}Tl, respectively) were calibrated relative to previous measurements in the Oxford and the Gif-sur-Yvette blocks (Richter et al., 2003) to obtain apparent parent element concentrations for K, Th, and U, assuming equilibrium in the ^{232}Th and ^{238}U series (Marques et al., 2021). The dose rate was determined through a combination of techniques. For the three sediment samples from Menga (Menga 2 Socket, Menga 1 Infill, and Menga 1 Contact), the dose rate was derived from in situ gamma measurements using a gamma spectrometer (HPI Rainbow MCA with a 3 inch x 3 inch NaI probe), performed in the sampling contexts. Stripped counts in the windows 1380–1530 keV, 1690–1840 keV, and 2550–2760 keV (designed to obtain signals dominated by ^{40}K, ^{214}Bi, and ^{208}Tl respectively) were calibrated relative to previous measurements in the Oxford and the Gif-sur-Yvette blocks (Richter et al., 2003) to obtain apparent parent element concentrations for K, Th, and U, assuming equilibrium in the ^{232}Th and ^{238}U series (Marques et al., 2021). The dose rate for the two sediment samples from El Toro (CET-OSL2 and CET-OSL3) was determined from the radionuclide activity concentration measured by high-resolution gamma spectrometry (Xtra HpGE spectrometer).

In addition, OSL was measured on six ceramic samples from various locations at the dolmen's atrium to further refine Menga's temporality (Table 5). For the ceramic shards, the dose rate was derived from the concentration of radioelements in the pieces (measured by inductively coupled plasma mass spectrometry) used to calculate the beta contribution and in situ gamma measurements for the gamma contribution to the dose rate.

U/Th dating

To further examine the age of the collapse of El Toro roof slab (and, indirectly, the abandonment of the cave and its possible relationship with the construction of Menga), four samples (designated as ET-1, ET-2, ET-3, and ET4 in Table 6) of calcite for U/Th dating were obtained from the present-day roof of the cave, just above the fallen slab. These samples were intended to provide additional *ante quem* ages for the collapse of the slab. However, these samples failed quality control, as they were all contaminated by detrital Th to a degree that accurate and precise U/Th ages could not be calculated. Detrital, or initial, ^{230}Th can be incorporated into speleothems when they form and may impact on the accuracy of the resulting U/Th age (Hoffmann et al., 2016). Typically, this is identified by measuring levels of ^{232}Th in the sample, and a correction can be applied, provided the isotopic composition of the detrital particles is well known and the contamination is not too severe. However, when $(^{230}Th/^{232}Th)_A$ is <20, the detrital Th corrections have a significant effect on the calculated ages, and with the four El Toro U/Th samples being characterized by $(^{230}Th/^{232}Th)_A \leq 1$ (Table 6), it was not possible to calculate accurate and precise U/Th ages.

Given that U/Th could not be used to directly date the collapse of the El Toro roof slab, a decision was made to take additional samples for U/Th dating from the El Aguadero sinkhole (Periana, Málaga), located some 60 km east of Antequera as the crow flies. A previous radiocarbon date (Beta-222473) on a calcite

Table 5. Optically stimulated luminescence (OSL) ages for pottery shards from Menga.

Lab code	Context	Dose rate (Gy/ka)			Equivalent dose (Gy)			Age (ka before 2016)			Calendar age
ANT-C-02	Atrium	2.64	±	0.18	2.20	±	0.03	0.83	±	0.06	1166 ± 60 CE
ANT-C-03	Atrium	2.23	±	0.21	4.50	±	0.09	2.02	±	0.19	4 ± 190 BCE
ANT-C-04	Atrium	3.54	±	0.26	12.00	±	0.11	3.39	±	0.25	1374 ± 250 BCE
ANT-C-05	Atrium	3.48	±	0.29	4.14	±	0.07	1.19	±	0.10	AD 826 ± 100
ANT-C-06	Atrium	2.49	±	0.25	13.14	±	0.17	5.27	±	0.53	3254 ± 530 BCE
ANT-C-07	Atrium	2.98	±	0.35	5.93	±	0.09	1.99	±	0.24	26 ± 240 BCE

https://doi.org/10.1017/qua.2022.33 Published online by Cambridge University Press

Table 6. U and Th concentrations, isotopic activity ratios and U-Th ages for the El Toro and El Aguadero speleothems.[a]

Lab ID	Sample ID	Description	^{238}U (ng/g)	±	^{232}Th (ng/g)	±	$(^{230}Th/^{232}Th)$	±	$(^{230}Th/^{238}U)$	±	$(^{234}U/^{238}U)$	±	Corrected age (ka)	Age error +	Age error −	$(^{234}U/^{238}U)_{initial}$	±
UoS-UTh-A120	ET-1	—	52.8	0.2	40.41	0.27	0.6200	0.0060	0.1554	0.0018	1.1028	0.0020	—	—	—	—	—
UoS-UTh-A121	ET-2	—	61.9	0.3	136.50	0.90	0.7230	0.0045	0.5214	0.0043	1.0934	0.0017	—	—	—	—	—
UoS-UTh-A122	ET-3	—	402.2	1.9	933.78	6.18	1.4272	0.0085	1.0841	0.0082	1.0109	0.0015	—	—	—	—	—
UoS-UTh-A123	ET-4	—	96.6	0.5	198.31	1.38	0.6201	0.0043	0.4165	0.0035	1.1685	0.0019	—	—	—	—	—
UoS-UTh-A286	C1-1a	161 mm from top	55.2	0.3	0.74	0.01	99.8475	1.8422	0.4402	0.0095	1.0674	0.0532	57.25	4.64	4.12	1.0795	0.0619
UoS-UTh-A287	C1-1b	59 mm from top	81.5	0.4	0.87	0.01	55.7480	1.1092	0.1935	0.0044	1.0909	0.0263	20.96	0.82	0.76	1.0967	0.0278
UoS-UTh-A288	C1-1c	40 mm from top	71.4	0.4	0.05	0.01	159.8043	35.7477	0.0343	0.0047	1.0530	0.0361	3.59	0.52	0.51	1.0535	0.0364
UoS-UTh-A289	C1-2a	186 mm from top	69.8	0.4	6.49	0.05	4.9193	0.1369	0.1496	0.0042	1.1234	0.0386	13.17	1.38	1.29	1.1313	0.0409
UoS-UTh-A290	C1-2b	151 mm from top	83.3	0.4	2.01	0.01	15.1661	0.3537	0.1199	0.0031	1.1100	0.0239	11.82	0.54	0.53	1.1144	0.0248
UoS-UTh-A291	C1-2c	22 mm from top	68.1	0.3	1.69	0.01	10.3648	0.4890	0.0844	0.0040	1.0834	0.0339	8.18	0.63	0.59	1.0859	0.0349

[a]Analytical errors are 2σ of the mean. $(^{230}Th/^{238}U) = 1 - e^{-\lambda 230 T} + (\delta^{234}U_{measured}/1000)[\lambda_{230}/(\lambda_{230} - \lambda_{234})](1 - e^{-(\lambda 230 - \lambda 234)T})$, where T is the age. Decay constants are 9.1705×10^{-6} a^{-1} for ^{230}Th, $2.8221 - 10^{-6}$ a^{-1} for ^{234}U (Cheng et al., 2013), and $1.55125 - 10^{-10}$ a^{-1} for ^{238}U (Jaffey et al., 1971). The degree of detrital ^{230}Th contamination is indicated by the measured $[^{230}Th/^{232}Th]$ activity ratio. Age corrections use an assumed detrital $(^{232}Th/^{238}U)$ of 1.250 ± 0.625, a value typical of upper crustal silicates (Wedepohl, 1995), while assuming ^{230}Th and U isotopes are in equilibrium.

sample from a stalactite of this cavity had suggested a possible earthquake dating to 5110 ± 70 cal yr BP (4045–3713 BCE [2σ]) (Clavero Toledo, 2010, p. 136; Bradley and García Sanjuán, 2017), which potentially matched the earthquake that, according to the excavators, had led to the abandonment of El Toro.

Thus, six U-Th dates were obtained from three speleothems (stalagmites) of El Aguadero with morphological features indicative of reorientations of growth resulting from possible tectonic movement (Becker et al., 2006; Kagan et al., 2005; see Fig. 6 and Tables 6 and 7 in which U and Th concentrations, isotopic activity ratios, and U-Th ages are presented). The El Aguadero stalagmite samples were sectioned using an electric bench saw to reveal fresh surfaces, then individual calcite layers were hand-drilled to produce powders for dating. Chemical preparation and isotopic analysis using a Thermo Scientific Neptune multicollector inductively coupled plasma mass spectrometer was performed at the Ocean and Earth Science analytical geochemistry facilities at the University of Southampton. The analytical methods are detailed in Hoffmann et al. (2018). Procedural chemistry blank values were always less than 0.01ng ^{238}U, 0.1 pg ^{235}U, 0.01 pg ^{234}U, 0.01ng ^{232}Th, and 1 fg ^{230}Th, respectively. A secular equilibrium standard, uraninite URAN 84.5, demonstrates both accuracy and external reproducibility of the analytical setup. Analyses gave the following activity ratios: $(^{230}Th/^{238}U) = 1.0026 \pm 0.0007$ and $(^{234}U/^{238}U) = 1.0001 \pm 0.0002$ (errors are given as 2σ standard errors of the mean, n = 50 over an ~1.5 year period). This is comparable to the values published for the same solution (Hoffmann et al., 2007). Analyses of a dissolved pristine speleothem sample served as an internal standard solution to further demonstrate external reproducibility. Analyses provided the following values: $(^{230}Th/^{23}8U) = 0.4335 \pm 0.0082$, $(^{234}U/^{238}U) = 1.0462 \pm 0.0053$, age = 58.15 ± 1.45 ka (errors are given as 2σ standard deviations of the mean, n = 14 over an ~1 year period).

RESULTS

Menga

Based on the radiocarbon dates described earlier, two Bayesian models were calculated for the construction of Menga (full data for all Bayesian models presented in this paper are available in the Supplementary Data files). The first combined 11 of the available dates (excluding Beta-526347, as it is much more recent and probably belongs to a later constructive phase) with the only date available for the Viera dolmen (GrN-16067: 4550 ± 140 cal yr BP),[2] built a few meters to the southwest of Menga. The Viera date acted as an *ante quem* date for the construction of Menga.[3] As a result, a robust model was obtained ($A_{model} = 96$) in which the construction of Menga has an early boundary in 3835–3715 BCE (1σ) or 3910–3660 BCE (2σ) (μ = 3785 BCE) and a late boundary in 3575–3500 BCE (1σ) or 3610–3450 BCE (2σ) (μ = 3530 BCE), with a span of 145–275 years (1σ) or 55–335 years (2σ) (Fig. 7A). This model introduced a function interval between Phase 1 (construction of Menga) and Phase 2 (Viera *ante quem* date) that yielded the following results: 0–215 years (1α) and 0–455 years (2α). The second model used the same 11

[2]Although this date presents a very high standard deviation, it is used here because it is the only one available to date the construction of this dolmen.

[3]This assumption is based on the observation that the stones of Menga must have been transported directly across the Viera location in their short trip from the quarries, which suggests Viera was built after Menga; see discussion in Lozano Rodríguez et al. (2014) and García Sanjuán and Lozano Rodríguez (2016).

https://doi.org/10.1017/qua.2022.33 Published online by Cambridge University Press

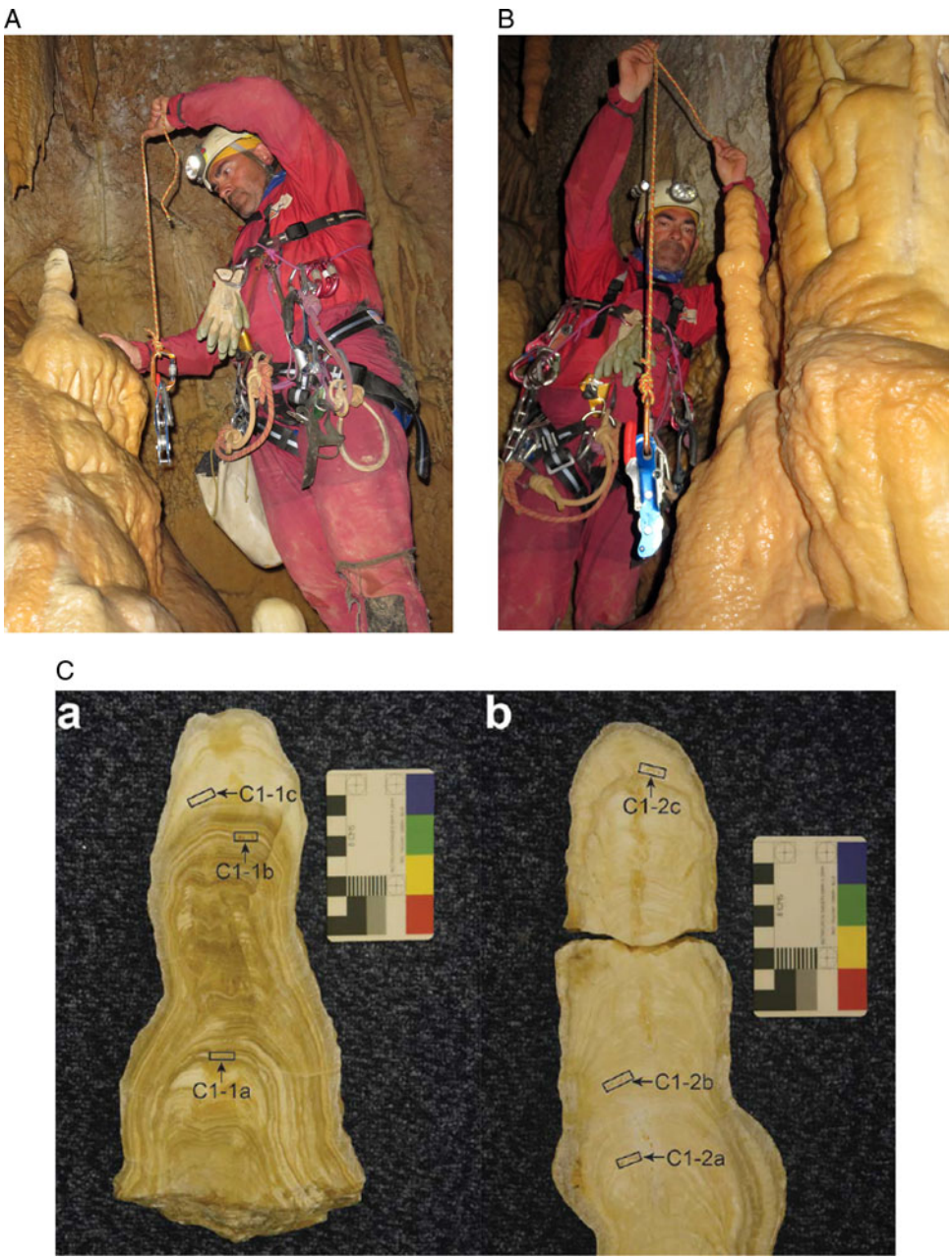

Figure 6. El Aguadero: (A) Stalagmite C1-1 in situ; (a) Stalagmite C1-1 after cutting; (B) Stalagmite C1-2 in situ; (b) Stalagmite C1-2 after cutting. (Photographs: A and B by JLCT; a and b by CDS.)

Menga dates, but in this case, date Beta-526347 from Sector E of Trench 1, clearly posterior to the rest of the dates, was used as the *ante quem* limit. As a result, an equally robust model was obtained ($A_{model} = 97$) in which the construction of Menga has an early boundary in 3825–3715 BCE (1σ) or 3895–3660 BCE (2σ) (μ = 3775 BCE) and a late boundary in 3575–3505 BCE (1σ) or 3610–3460 BCE (2σ) (μ = 3535 BCE), with a span of 140–265 years (1σ) or 55–315 years (2σ) (Fig. 7B). This model also introduced a function interval between Phases 1 and 2 with the following results: 0–165 years (1α) and 0–315 years (2α). In summary, the results of these two models set the construction of Menga between ca. 3900 and 3500 BCE (2σ).

The radiocarbon-based chronometric models obtained for Menga were then compared with the three OSL ages obtained from samples of the infill of the socket of Pillar 3 (Fig. 4, Table 2), according to the reasoning described earlier. The sediments from inside the socket of Pillar 3 yielded the following OSL ages: 5.8 ± 0.3, 5.5 ± 0.4, and 5.5 ± 0.8 ka (or 3769 ± 201, 3517 ± 325 and 3543 ± 510 BCE) (Table 2). These three ages are very consistent with each other within 1σ and with the results of the Bayesian models described earlier, giving robustness to the results of the radiocarbon dating and making it possible to establish that the construction of Menga took place between c. 3800 and 3600 BCE. These three new OSL dates are the first ever obtained for the Antequera megalithic site, and save for a "para-megalithic" structure located in Carmona, Sevilla, dating to antiquity (Athanassas et al., 2017), they are the first ones ever published for an Iberian megalithic chamber.

https://doi.org/10.1017/qua.2022.33 Published online by Cambridge University Press

Table 7. Summary data for uranium-thorium determinations for possible earthquakes at El Aguadero sinkhole.

Sample code	Sample provenance	Lab code	Corrected age (ka)	Age error +	Age error −
C1-1	From cluster of speleothems located on the eastern side of the chamber. The general orientation of the wall is 0°N. Active stalagmite (with humidity), 25 cm in length.	UoS-UTh-A286 (sample ID C1-1a)	57.25	4.64	4.12
		UoS-UTh-A287 (sample ID C1-1b)	20.96	0.82	0.76
		UoS-UTh-A288 (sample ID C1-1c)	3.59	0.52	0.51
C1-2	From cluster of speleothems located on the eastern side of the chamber. The general orientation of the wall is 0°N. Very active stalagmite (very humid, frequent dripping), 50 cm in length.	UoS-UTh-A289 (sample ID C1-2a)	13.17	1.38	1.29
		UoS-UTh-A290 (sample ID C1-2b)	11.82	0.54	0.53
		UoS-UTh-A291 (sample ID C1-2c)	8.18	0.63	0.59

In addition, the estimated ages for the six ceramic fragments obtained at various locations in Menga's atrium (Table 3) show rather disparate ages variously set in the Late Neolithic, Bronze Age, antiquity, and Middle Ages. While reflecting the long biography of the monument, these ages are quite important, precisely because they demonstrate how consistent and tight the radiocarbon chronology of the materials recovered from the mound is, which is of crucial value to ensure the reliability of the proposed date for Menga's construction.

Altogether, combining the results of the radiocarbon and OSL dates, it is possible to narrow down the probable construction date of Menga to between ca. 3800 and 3600 BCE. Those freshly obtained numerical ages provide a high-resolution empirical base to understand the social and cultural background surrounding the construction of this exceptional dolmen, as will be discussed later.

El Toro Cave

Establishing the degree of synchronicity between the abandonment of El Toro and the building of Menga was also a major aim of this study. To this end, three Bayesian models were made to establish the time of the collapse of El Toro Cave's roof slab. Several determinations already published for this cave (Egüez et al., 2016) were discarded, including those dating Early Neolithic activity, which are not relevant in this case (Beta-174305, UGRA-194, GrN-1544, Beta-174308, Beta-341132, Beta-341131, GrN-15444, and GrN-15440) and those dating sporadic frequentation after its abandonment. Other dates were discarded on account of the low quality of the samples or standard deviations above 100 years (GrN-15446, UGRA-189, I-17533, I-17532, Gak-8060, and Gak-8059).

The first model, based on the selected 15 radiocarbon determinations, was not statistically robust ($A_{model} = 38$). A second model, calculated on the basis of 14 determinations, excluding Beta-174307, which is later than the rest of the series, was statistically robust ($A_{model} = 95$). This model shows that the end of the cave's occupation had an early chronological boundary set between 4175 and 4050 BCE (1σ) or between 4250 and 4045 BCE (2σ) (μ = 4125 BCE) and a late chronometric boundary set between 4030 and 3965 BCE (1σ) or between 4050 and 3935 BCE (2σ) (μ = 3995 BCE), with a span of 20–155 years (1σ) or 0–240 years (2σ) (Fig. 7C). According to the 2σ intervals, the abandonment of the cave would have occurred between 4250 and 3935 BCE.

Next, we used the three newly obtained radiocarbon determinations to try to establish the date of the collapse of the roof slab (Table 5). Date Beta-428896, obtained from a sample from underneath the slab, provided an age for the latest activity in the cave before the fall of the slab. The two dates from above the slab (Beta-429656 and Beta-428897) were not statistically identical. For this reason, a model was calculated with two sequential phases: the first phase incorporates date Beta-428896 and latest of the two dates from above the slab (Beta-336259), while the second phase includes both dates from above the slab. The resulting model is on the threshold of being statistically robust ($A_{model} = 60$), and for the phase before the fall of the slab (Phase 1), it provides an early boundary between 5000 and 4705 BCE (1σ) or between 5630 and 4620 BCE (2σ) (μ = 4955 BCE) and a late boundary set between 4140 and 3980 BCE (1σ) or between 4160 and 3965 BCE (2σ) (3955 BCE), while for the phase after the collapse of the roof slab (Phase 2), it yields an early boundary set between 4025 and 3970 BCE (1σ) or between 4110 and 3855 BCE (2σ) (μ = 4010 BCE) and a late boundary set between 3960 and 3795 BCE (1σ) or between 3980 and 3510 BCE (2σ) (μ = 3825 BCE), with an interval between Phase 1 and Phase 2 of 0–40 years (1σ) or 0–120 years (2σ). Therefore, if we take the late boundary of Phase 1 and the early boundary of Phase 2, the roof slab fell between 4160–3965 and 4110–3855 BCE (2σ), which is highly consistent with the results of the model based on the already published dates for El Toro, as described earlier.

Finally, a third Bayesian model was calculated in which the published dates for the occupation of the cave (Phase 1) were combined with the new dates for the time *after* the collapse of the roof slab (Phase 2). The resulting model (Fig. 7D) was robust ($A_{model} = 79.3$) and set the early boundary of the cave's abandonment (Phase 1) between 4160 and 4050 BCE (1σ) or between 4180 and 4000 BCE (2σ) (μ = 4095 BCE) and the late boundary for it between 4045 and 4000 BCE (1σ) or between 4155 and 3975 BCE (2σ) (μ = 4030 BCE). The sporadic activity after the collapse of the roof slab has an early boundary between 4020 and 3975 BCE (1σ) or between 4070 and 3955 BCE (2σ) and a late boundary between 3970 and 3870 BCE (1σ) or 3985 and 3685 BCE (2σ), with an interval of 0–35 years (1σ) or 0–105 years (2σ). Choosing to err on the side of caution, we combined the early boundary of the cave's abandonment with the late boundary of the sporadic activity after the collapse of the slab: in that case, the cave was abandoned between 4160 and 3870 BCE (1σ) or between 4180 and 3685 BCE (2σ).

In summary, the Bayesian model calculated on the basis of the previously published dates, shows that the end of El Toro's sequence of permanent occupation occurred between 4250 and 3935 BCE (2σ). A Bayesian model based on the three new radiocarbon determinations obtained by us from sediments below and

https://doi.org/10.1017/qua.2022.33 Published online by Cambridge University Press

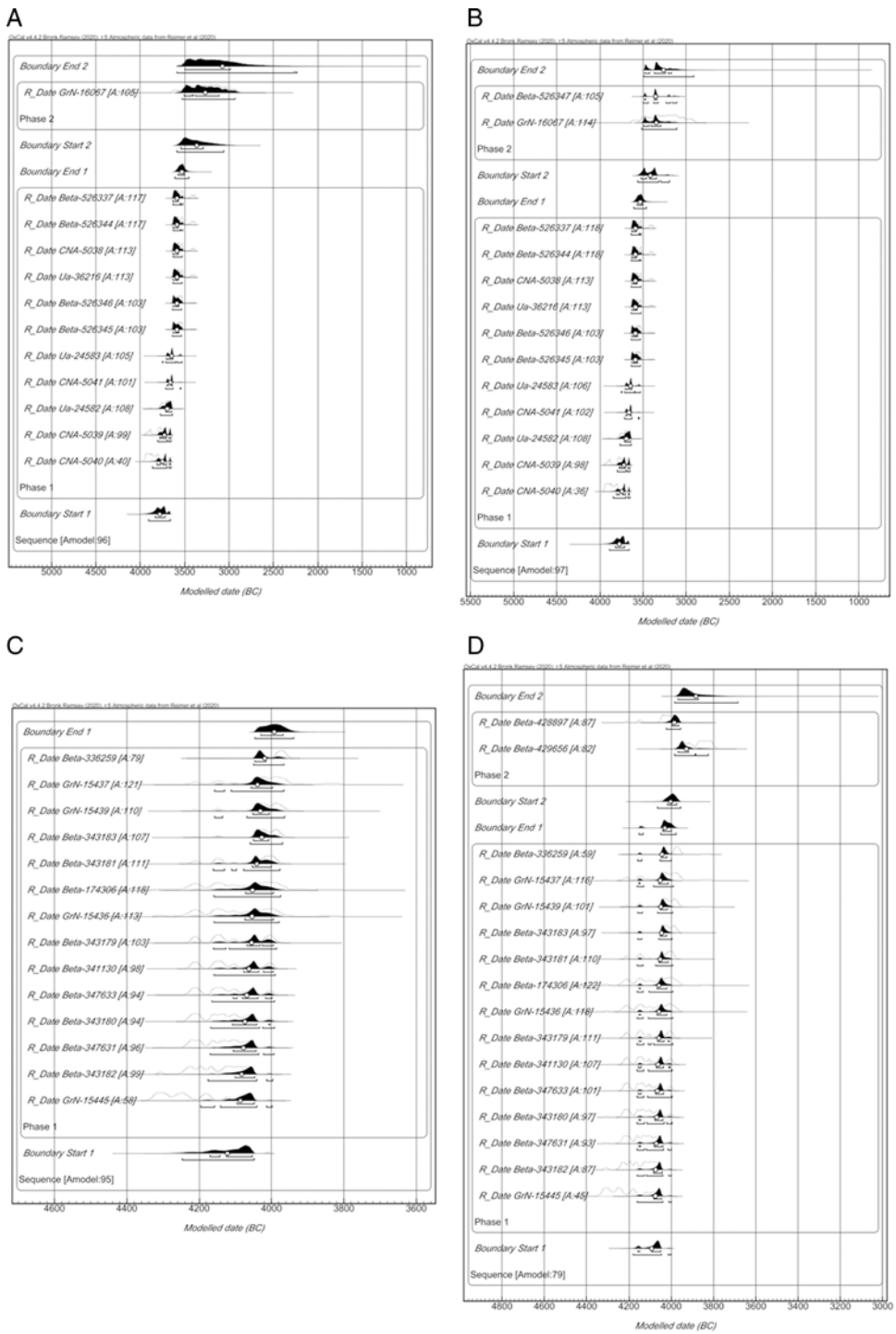

Figure 7. Bayesian models for Menga and El Toro: (A) construction of Menga: Menga and Viera dates; (B) construction of Menga: all Menga dates; (C) abandonment of El Toro: published dates; (D) abandonment of El Toro: published dates and new dates for the fallen roof slab. (Design: VBN and LGS.)

above the fallen slab showed that the fall of the slab occurred between 4110 and 3510 BCE (2σ), whereas a mixed model combining the previous two models (including both published and new dates) revealed the cave was very probably abandoned between 4180 and 3685 BCE (2σ).

These results were then compared with the two OSL ages from sediments from below and above the El Toro's fallen roof slab (Fig. 8, Table 2). The sample from underneath the slab (CET-OSL3) provided an age of 5.1 ± 0.3 ka (or 3113 ± 164 BCE), while the one from above the slab (CET-OSL2) returned an age of 4.8 ± 0.3 ka (or 2781 ± 166 BCE). The corresponding dose distributions are shown in Figure 8. Although congruent between themselves, these ages do not consistently match the ones provided by the radiocarbon samples. This may have been caused by unaccounted-for postdepositional activity in those sediments. Despite the failure of U-Th samples and lack of accordance between the OSL ages and the radiocarbon ages, the radiocarbon models reveal that the collapse of El Toro's roof slab and subsequent end of the stable

https://doi.org/10.1017/qua.2022.33 Published online by Cambridge University Press

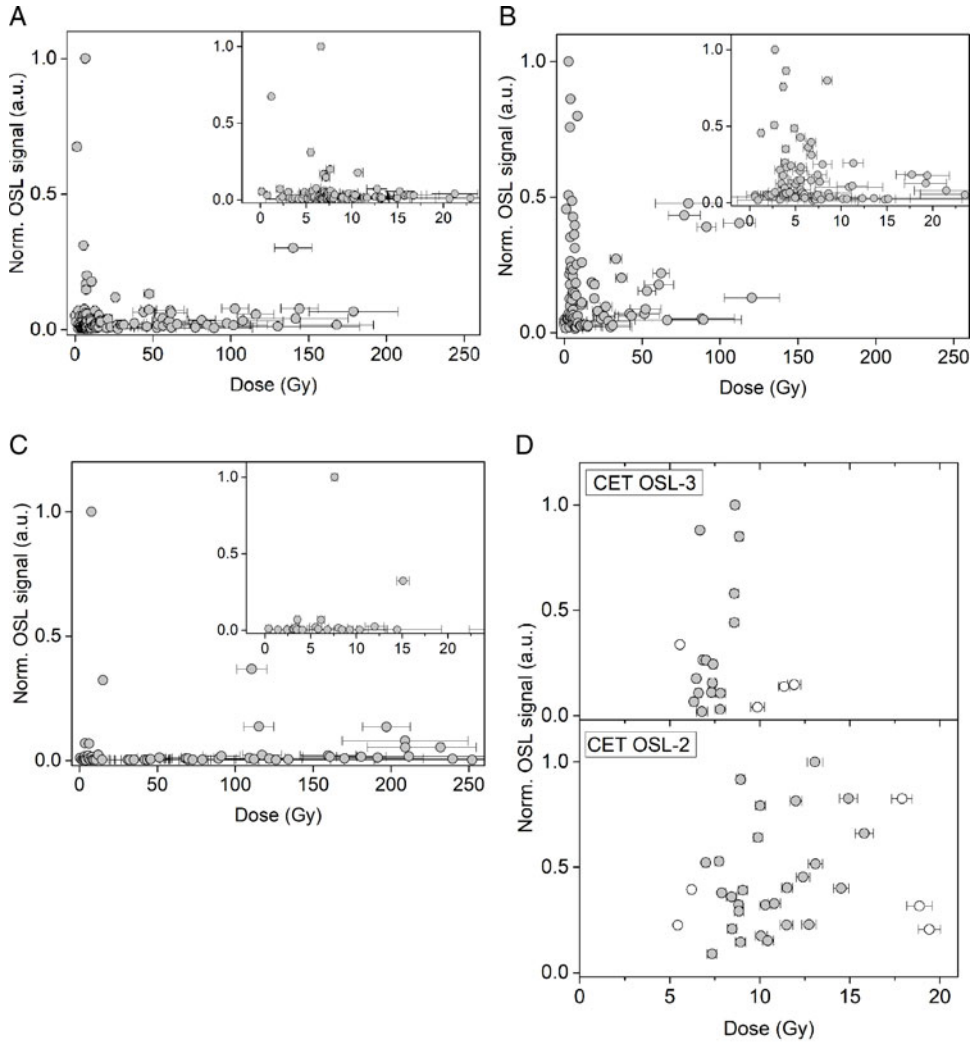

Figure 8. (A–C) Menga: dose distributions of samples from Menga derived from optically stimulated luminescence (OSL) measurements of quartz single grains. The plots show the individual dose values and their uncertainties. (D) El Toro: dose distributions of samples derived from OSL measurements of quartz multigrain aliquots.

occupation of the cave were coeval, both having occurred shortly before (or at the time of) the construction of Menga.

To explore whether the El Toro roof slab fell as a result of an earthquake, six samples from two stalagmites collected from El Aguadero sinkhole were dated. Three samples from stalagmite C1-1 (Fig. 6Aa) produced ages from 57.25 (+4.64, −4.12) ka (C1-1a) to 3.59 (+0.52, −0.51) ka (C1-1c). Growth therefore commenced in or before the late Middle Paleolithic and continued to some degree well into the Holocene. Sample C1-1c formed during later prehistory, around the Middle Bronze Age and Late Bronze Age transition. Sample C1-1b, located 19 mm nearer to the base of the stalagmite, dates to 20.96 (+0.82, −0.76) ka, and with no clear shift in the axis of growth between these two samples, there is no clear evidence of stalagmite realignment due to tectonic activity in the Neolithic. Three samples from stalagmite C1-2 (Fig. 6 Bb) produced ages from 13.17 (+1.38, −1.29) ka (C1-2a) to 8.18 (+0.63, −0.59) ka (C1-2c). Sample C1-2c is located 22 mm from the top of the stalagmite; therefore, the vast majority of growth occurred before the Neolithic. The obvious shift in the growth axis of this stalagmite (seen toward the bottom of the image) occurred between samples C1-2a and C1-2b, so between 11.29 ka and 14.55 ka. The results show that none of the six El Aguadero U/Th ages obtained as part of this study record an earthquake in the Antequera region matching the results of radiocarbon date Beta-222473 published by Clavero Toledo (2010, p. 136).

DISCUSSION: BIRTH OF A GIANT

Once a reliable date for the construction of Menga is available, it becomes possible, for the first time, to analyze the social and cultural background of its genesis, at both the local and regional scales. Synthetic ages summarizing the data described earlier are provided in Table 8.

In terms of the local scale, the construction of Menga between ca. 3800 and 3600 BCE is set against the background of major social and cultural changes at the start of the Late Neolithic period (spanning ca. 4200 to 3200 BCE). One of those changes was

https://doi.org/10.1017/qua.2022.33 Published online by Cambridge University Press

Table 8. Summary results of chronometric models for El Toro cave and Menga.

Event	Age BCE 2σ
End of El Toro sequence according to published dates	Between 4250–4045 and 4050–3935
Collapse of El Toro roof slab	Between 4160–3965 and 4110–3855
Abandonment of El Toro (combined)	4180–3685
Construction of Arroyo Saladillo burial 94 (after García Sanjuán et al., 2020)	4037–3805
Construction of Menga (date Viera GRN-16067 as *ante quem*)	Between 3910–3660 and 3610–3450
Construction of Menga (date Menga Beta-526347 as *ante quem*)	Between 3895–3660 and 3610–3460
Construction of Menga (optically stimulated luminescence) dates)	3769 ± 201 3543 ± 510 3517 ± 325

undoubtedly the abandonment of the "ancestral" El Toro cave between 4180 and 3685 BCE (2σ). While the data presented here cannot falsify the "earthquake hypothesis" and future speleoseismological research dedicated to cave surveys and speleothem sampling across the region could provide further evidence to establish whether or not a major earthquake occurred ca. 4100–3900 BCE, other explanations can be found to account for the collapse of the roof slab at El Toro. Within El Torcal, the limestone massif in which El Toro is located, a very intense fracturing is recognized in relation to two conjugated systems whose directions are 40°N–60°E and 110°N–120°E respectively (Burillo Panivino, 1998). This formation is based on a pseudo-horizontal stratigraphy, which clearly conditions the circulation of water, helping the dissolution of the various materials that form it (well-stratified oolithic, nodular, or pseudobrechoid limestones arranged in boards or banks ranging from a few centimeters to 3–4 m). Karstic corridors, sinkholes, and caves, among other geomorphological features, are thus formed. Due to their different textures and carbonate content, the limestones of the massif have allowed differential action of external agents (dissolution, gelation, and perhaps wind action) on the strata, with alternating and well-defined characteristics in the upper part of the massif (Burillo Panivino, 1998). This alternation of limestones with different responses to dissolution and tectonic fracturing within the karstic massif generates differentiated blocks on the roof of its caves. Over time, they may fall due to gravity, which may, in some cases, be helped by seismic activity. In the case of El Toro, it is important to add that the very same anthropogenic activity starting inside the cave at the onset of the Early Neolithic (ca. 5400 BCE), with an obvious increase of CO_2 concentrations (caused by hearths and other combustion activities) must have helped the dissolution of carbonate blocks, leading to the potential collapse of roof slabs by gravity.

Altogether, the sudden abandonment of the cave, most likely caused by the catastrophic collapse of the roof slab, must have resonated across the region. At that time, intense human activity was already taking place at various locations on the Antequera plain. This included the northern sector of La Peña de las Enamorados, where the Matacabras rock art sanctuary, the exact spot to which Menga's axis of symmetry is oriented, was in use before ca. 3800 BCE (Rogerio-Candelera et al., 2018), and Arroyo Saladillo, located 6 km to the west of Menga, where an individual inhumation (Structure 94) was made in 4037–3805 BCE (2σ) and covered by a cairn of medium-to-large stones, probably in combination with a ditch (García Sanjuán et al., 2020). This tomb is one of Iberia's earliest proto-megalithic graves, which is of the greatest interest in the context of Menga's genesis. Large amounts of knapped lithics and grinding tools found at both Arroyo Saladillo and Huerta del Ciprés (located barely 700 m to the north of Menga) also reveal an intensification of farming activity across the region, with a growing anthropogenic impact (García Sanjuán et al., 2020). Therefore, the construction of Menga was preceded by a buildup or formative phase in which expanded farming, exploitation of abiotic resources (particularly salt, flint, and volcanic rocks, abundant in the region; Lozano Rodríguez et al., 2010, 2014, 2018a, 2018b; Morgado Rodríguez and Lozano Rodríguez 2011, 2012; Lozano Rodríguez and Morgado Rodríguez, 2012; Morgado Rodríguez et al., 2013), exchange (based on a privileged network that relied on Antequera's geographic position at a major crossroads), and ritual activity at La Peña's northern sector played a major part.

While entirely consistent with the construction of a monument as massive as Menga, this activity does not appear to have included any major stone structures. In other words, a striking paradox becomes apparent: no precedents for an architecture as colossal as Menga existed in the Antequera region, or indeed in Iberia as a whole, in the centuries leading up to its construction. The only megalithic monument known locally before the construction of Menga is Structure 94 at Arroyo Saladillo, which is far smaller and undoubtedly required a very different scale of labor and technological expertise. On the basis of the newly available chronology for its construction, Menga appears to have sprung as an incredible feat of engineering from a background of very little or no previous megalith-building tradition. This raises an important question: where did the builders of Menga draw their formidable expertise from? Two possible hypothetical answers can be given to this question.

The first hypothetical answer lies in the production and emplacement of menhirs. In numerous regions of Iberia there is consistent evidence of "open" monumental sites with menhirs that predate the construction of megalithic burial chambers. This is especially the case in the Alentejo and Algarve regions, in southern Portugal (Calado, 2004, 2006; Cerrillo Cuenca et al., 2019), but also in northern Spain (Peñalver Iribarren, 1989, 2011; Martínez Torres, 2015). These monuments offer a wide variety of situations, ranging from a large number of medium-sized stones, as is the case in the Almendres cromlech, with about 100 stones, or a smaller number of bigger stones, as occurs at Meada (Portalegre, Alentejo), where a single menhir is 7.5 m in height and weighs an estimated 18 tons, most likely the largest of its kind in Iberia. Although they are generally dated to the fifth millennium BCE, their chronology of foundation and use is quite poorly known. There are two reasons for this: first, very little or no burial activity took place around them, and therefore no radiocarbon dates on human bone are available; second, no OSL dates dating their construction have been obtained, save for some very specific exceptions, which have high standard error margins or await confirmation.

Did the builders of Menga gain their expertise in the handling of massive stones through earlier menhir-making? The possible presence of menhirs was suggested for the site of Piedras Blancas, at the northern sector of La Peña de los Enamorados (García Sanjuán et al., 2015), but while recent excavations have ruled out this possibility for some of the stones lying there, good-quality dating is still needed for others. The same applies to

https://doi.org/10.1017/qua.2022.33 Published online by Cambridge University Press

suggestions that some of Menga's stones were first used as menhirs or stelae, probably at the very same location of the dolmen, and then reused as uprights and capstones when Menga was built (Bueno Ramírez et al., 2009, p. 191). In principle, this hypothesis is consistent with the recent discovery of wine among the residues preserved in the pottery shards found in the mound of the dolmen, which, as was explained earlier, predate its construction (Garnier et al., 2022). Wine was likely associated with practices of feasting, conviviality, and commensality, which are typical of societal gatherings such as those taking place at monumentalized sites in the Late Neolithic. In this "menhir hypothesis," the construction date of Menga as a dolmen would have been different (i.e., later) than that of the making of some of its stones, which would add another layer of difficulty to the reconstruction of its complex biography.

Another hypothetical explanation of the apparent lack of local precedents for the construction of Menga is human mobility. This hypothesis sets this monument against the background of the various cultural phenomena occurring in the Iberian Peninsula in the early fourth millennium BCE, that is to say, at the onset of the Late Neolithic period, including the abandonment of caves for open-air settlements, the generalization of ditched enclosures, and the spread of megalithic chambers. A phenomenon clearly associated with this period is an increase in supraregional human interaction. Recent studies have revealed the presence of variscite from Huelva (southwest Spain, 200 km west of Antequera) in the Carnac region of French Brittany since ca. 4500 BCE and from Palazuelo de las Cuevas (Zamora, in the Spanish central plateau) since 4300–4000 BCE (Querré et al., 2019). From ca. 4700 BCE, evidence of large-scale megalithic monumentality exists in various regions of western France (Guilaine, 2011, pp. 79–81). Throughout the Atlantic façade, and more particularly in Brittany, "low" burial mounds with block enclosures including small, closed chambers (called *coffres* in French literature) are known, although the most impressive monuments are undoubtedly the gigantic burial mounds from the Carnac region (Saint-Michel, Le Moustoir, and Tumiac), ranging between 100 and 200 m in length, which in all cases cover a central tomb built in stone blocks, sometimes with corbelled roofing. In Brittany from ca. 4500 BCE, there is also evidence of large menhirs, stelae, and menhir-statues, some of which were later reused in megalithic burial chambers. In the Orleans region, single or double tombs covered by imposing stone slabs, attributed to the Cerny-Videlles cultural complex, were built around 4600–4500 BCE. According to the currently available radiocarbon data, all these cases predate by several centuries the appearance of the first proto-megalithic burial chambers in the Iberian Peninsula, around 4200–4000 BCE (García Sanjuán et al., 2022), and certainly the construction of the Menga dolmen between 3800 and 3600 BCE. In the absence of better data on Portuguese and North African megalithic chambers, for which there are still no precise radiocarbon series to help understand their oldest developments, if one is to seek a "foreign inspiration" for the constructive genius implicit in the dolmen of Menga, the most obvious reference is Atlantic France.

Whether the fifth millennium BCE direct contacts between France and Iberia suggested by the variscite occurred by land or sea is at present unknown. The possibility of long-range maritime voyaging along the Atlantic Seaboard during the Late Neolithic has been suggested repeatedly (Callaghan and Scarre, 2017; Cassen et al., 2019; Schulz Paulsson, 2019). A recent analysis of the painted boats at Laja Alta (Cadiz) suggests sailing seafaring during the first half of the fourth millennium BCE (Morgado Rodríguez et al., 2018). This interaction between various Atlantic regions of Iberia and France was also the background to the "arrival" of the Neolithic in the British Isles, recently dated to ca. 4050 cal BCE (Whittle, 2018, p. 5), which obviously required seaworthy boats. Interestingly, recent aDNA analyses have shown that the genetic ancestry of early Neolithic settlers in the British Isles was closer to that of Iberian and Mediterranean populations than central European populations (Brace et al., 2019; Rivollat et al., 2020).

Therefore, within a supraregional scale of analysis, the construction of Menga occurred at a time of increased mobility and interaction between regions in Atlantic Europe, which may have led to the spread of proficiency in megalith-building techniques. Can the lack of precedents for a monument as fine and colossal as Menga be explained by the participation of "foreign" experts? At this time, and with the evidence available, this cannot be tested, but the newly established date for the inception of the monument opens up this possibility for future analysis. Only further research will help us to understand the apparent contradiction posed by Menga's uniqueness and perfection on the one hand, and the lack of obvious local precedents on the other.

What is beyond doubt, however, is that, upon its construction, Menga gained huge fame. Over time, it would act as a permanent focus of monumentality, ritual practice, and social action in the region. The Viera dolmen, as well as the recently discovered Piedras Blancas megalithic structure, both very likely built at the end of the fourth millennium, and El Romeral tholos, built sometime during the third millennium would have acted as "responses" provided by the local communities to the glorious past represented by the great Menga dolmen as a part of a powerful sense of place-keeping.

CONCLUSION

Through a careful combination of geological and archaeological observations, coupled with a multimethod approach based on 29 new radiocarbon, OSL, and U/Th numerical dates, an innovative and robust approach is made to a problem that for a long time was deemed as almost intractable: the establishment of the construction date of major megalithic monuments. Monumentality is one of the most challenging subjects in the study of early social complexity. The erection of monuments is closely linked to the rise and consolidation of the Neolithic way of life and associated phenomena, such as sedentarization, demographic growth, agricultural intensification, surplus accumulation, craft specialization, increased social and gender differentiation, ritual central places, political hierarchization, and supraregional connectivity. In Europe, major sites of ritual character involving massive earthen monuments (such a ditched enclosures and henges) and megaliths were built between the fifth and third millennia BCE, in what represents a remarkable era in human social evolution. In the case study examined here, not only is a fairly reliable date obtained for the construction of Menga, one the largest megalithic monuments in Europe, but significant information is also gathered regarding the circumstances that surrounded its construction almost 6000 years ago.

In addition to the importance this study has for our understanding of the Antequera monumental landscape, there are significant methodological lessons to be drawn from it. Systematic multimethod dating may and will encounter problems. In the case study presented here, this is reflected in the impossibility of dating calcite crusts from El Toro, the lack of consistency

https://doi.org/10.1017/qua.2022.33 Published online by Cambridge University Press

between the radiocarbon and OSL dates obtained for the fall of the El Toro roof slab, and the chronometric "noise" produced by the estimated ages of hand-thrown pottery from Menga's atrium. In addition, the "synchronization" of multiple ages based on a wide array of methods demands time, resources, and a significant amount of multidisciplinary expertise. Despite these problems, however, a multimethod approach can successfully contribute to the establishment of construction dates of major prehistoric monuments, which in turn is a sine qua non condition to comprehend the social and cultural backgrounds they emerged from and were part of.

Acknowledgments. This research presented in this paper was funded by two projects of the National R&D Plan of the Spanish Government: "Megalithic Biographies: The Antequera Megalithic Landscape in Its Temporal and Spatial Context" (HAR2017-87481-P, 2018-2021), and "Nature, Society and Monumentality: High-Resolution Archaeological Investigations of the Antequera Megalithic Landscape" (HAR2013-45149-P, 2014-2017). We would like to thank Francisco Crespo Fuillerat, Charo Moreno, Andrés Muñoz Martínez, Emilia Pérez Díaz, and Domingo Ruiz Canto of the Underground Exploration Group of the Sociedad Excursionista de Málaga for their contribution in obtaining the El Aguadero sinkhole speleothems. Grateful acknowledgments are also made to Fundação para a Ciência e a Tecnologia (FCT, Portugal), through the UID/Multi/04349/2020 and post-doctoral grant SFRH/BPD/114986/2016. We also thank Francisco Jiménez Espejo and José Antonio Lozano Rodriguez for their invaluable help while we were writing this paper, and Francisco Carrión Méndez for generously granting access to the records of his 2005-2006 excavations at Menga.

REFERENCES

Aitken, M.J., 1985. *Thermoluminiscence Dating*. Academic Press, London.

Aitken, M.J., 1999. Archaeological dating using physical phenomena. *Reports on Progress on Physics* **62**, 1333–1376.

Aranda Jiménez, G., García Sanjuán, L., Mora Molina, C., Moreno Escobar, M.C., Riquelme Cantal, J.A., Robles Carrasco, S., Vázquez Paz, J., 2015. Evidencias de asentamiento y prácticas funerarias en los dólmenes de Menga y Viera en la Antigüedad. La Intervención de 1988. *Menga. Revista de Prehistoria de Andalucía* **6**, 253–289.

Athanassas, C.D., García Sanjuán, L., Stamoulis, K., Lineros Romero, R., Carinou, E., Anglada Curado, R., 2017. Optically stimulated luminescence 1 (OSL) dating of an enigmatic, megalithic-like, subterranean structure in Carmona (Seville, Spain). *Journal of Archaeological Sciences Reports* **16**, 240–247.

Athanassas, C.D., Rollefson, G.O., Kadereit, A., Kennedy, D., Theodorakopoulou, K., Rowan, Y.M., Wasse, A., 2015. Optically stimulated luminescence (OSL) dating and spatial analysis of geometric lines in the northern Arabian desert. *Journal of Archaeological Science* **6**, 1–11.

Athanassas, C., García Sanjuán, L., Theodorakopoulou, K., Jain, M., Sohbati, R., Guerin, G., Lozano Rodríguez, J. A., 2016. Testing the potential of optically stimulated luminescence (OSL) for the dating of the Antequera megaliths (Málaga, Spain): assessing the results of the first round of sampling. *Menga: Revista de Prehistoria de Andalucía* **7**, 157–164.

Baceiredo Rodríguez, V., Baceiredo Rodríguez, D., García Sanjuán, L., Odriozola Lloret, C., 2014. Planimetría de alta resolución del dolmen de Menga (Antequera, Málaga) mediante escaneado láser terrestre, levantamiento 3D y fotogrametría. *Menga. Revista de Prehistoria de Andalucía* **5**, 259–269.

Becker, A., Davenport, C.A., Eichenberger, U., Gilli E., Jeannin, P.Y., Lacave, C., 2006. Speleoseismology: a critical perspective. *Journal of Seismology* **10**, 371–388.

Brace, S., Diekmann, Y., Booth, T., Van Dorp, L., Faltyskova, Z., Rohland, N., Mallick, S., *et al.*, 2019. Ancient genomes indicate population replacement in Early Neolithic Britain. *Nature Ecology & Evolution* **3**, 765–771.

Bradley, R., García Sanjuán, L. 2017: Sudden time? Natural disasters as a stimulus to monument building: from Silbury Hill (Great Britain) to Antequera (Spain). In: Bickle, P., Cummings, V., Hofmann, D., Pollard, J. (Eds.), *Neolithic Europe: Essays in Honour of Professor Alasdair Whittle*. Oxbow, Oxford, pp. 181–201.

Bronk Ramsey, C., 1995. Radiocarbon calibration and analysis of stratigraphy: the OxCal program. *Radiocarbon* **37**, 425–430.

Bronk Ramsey, C., 2009. Bayesian analysis of radiocarbon dates. *Radiocarbon* **51**, 337–360.

Buck, C.E., Cavanagh, W.G., Litton, C.D., 1996. *Bayesian Approach to Interpreting Archaeological Data*. Wiley, Chichester, UK.

Bueno Ramírez, P., De Balbín Behrmann, R., Barroso Bermejo, R., 2009. Análisis de las grafías megalíticas de los dólmenes de Antequera y su entorno. In: Ruiz González, B. (Ed.), *Dólmenes de Antequera. Tutela y Valorización Hoy*. Junta de Andalucía, Seville, pp. 186–197.

Burbidge, C.I., Trindade, M.J., Dias, M.I., Oosterbeek, L., Scarre, C., Rosina, P., Cruz, A., *et al.*, 2014. Luminescence dating and associated analyses in transition landscapes of the Alto Ribatejo, Central Portugal. *Quaternary Geochronology* **20**, 65–77.

Burillo Panivino, F.J., 1998. El karst del Torcal de Antequera. In: Durán, J.J., López Martínez, J. (Eds.), *Karst en Andalucía*. Instituto Tecnológico Geominero de España, Madrid, pp. 153–164.

Calado, D., 2003. Quinta da Queimada, Lagos, Portugal. Datação do momento de erecção de um monumento megalítico a través de Luminescência Óptica de cristais de quartzo (OSL). In: *Libro de Resúmenes del V Congreso Ibérico de Arqueometría (Puerto de Santa María, Cádiz, 2003)* [abstracts], pp. 167–168.

Calado, M., 2004. *Menires do Alentejo Central. Génese e Evolução da Paisagem Megalítica Regional*. Universidade de Lisboa, Lisbon

Calado, M., 2006. The menhirs of the Iberian Peninsula. In: Joussaume, R., Laporte, L., Scarre, C. (Eds.), *Origin and Development of the Megalithic Phenomenon of Western Europe. Proceedings of the International Symposium (Bougon, France, October 26th–30th 2002)*. Conseil Général de Deux Sèvres, Niort, France, pp. 613–636.

Callaghan, R., Scarre, C., 2017. Biscay and beyond? Prehistoric voyaging between two Finisterres. *Oxford Journal of Archaeology* **36**, 355–373.

Cassen, S., Fábregas Valcarce, R., Grimaud, V., Pailler, Y., Schulz Paulsson, B., 2019. Real and ideal European maritime transfers along the Atlantic coast during the Neolithic. *Documenta Praehistorica* **46**, 308–325.

Cerrillo Cuenca, E., Bueno Ramírez, P., Balbín-Behrmann, R., 2019. 3DMeshTracings: a protocol for the digital recording of prehistoric art. Its application at Almendres cromlech (Évora, Portugal). *Journal of Archaeological Science: Reports* **25**, 171–183.

Chapman, R.W., 1990. *Emerging Complexity. The Later Prehistory of South-East Spain, Iberia and the West Mediterranean*. Cambridge University Press, Cambridge.

Chapman, R.W., 1981. The emergence of formal disposal areas and the problem of megalithic tombs in Prehistoric Europe. In: Chapman, R.W., Kinnes, I., Randsborg, K. (Eds.), *The Archaeology of Death*. Cambridge University Press, Cambridge, pp. 71–82.

Cheng H., Edwards R.L., Shen C.-C., Polyak, V.J., Asmerom, Y., Woodhead, J., Hellstrom, J., *et al.*, 2013. Improvements in ^{230}Th dating, ^{230}Th and ^{234}U half-life values, and U-Th isotopic measurements by multi-collector inductively coupled plasma mass spectrometry. *Earth and Planetary Science Letters* **371–372**, 82–91.

Clavero Toledo, J.L., 2010. Investigación sísmica en simas de la alta Axarquía (Málaga): comportamiento de la falla que originó el terremoto de 1884. *Jábega* **102**, 130–140.

Egüez, N., Mallol, C., Martín Socas, D., Cámalich Massieu, M.D., 2016. Radiometric dates and micromorphological evidence for synchronous domestic activity and sheep penning in a Neolithic cave: Cueva de El Toro (Málaga, Antequera, Spain). *Archaeological and Anthropological Sciences* **8**, 107–123.

Galbraith, R.F., Roberts, R.G., Laslett, H., Yoshida, G.M., Olley, J.M., 1999. Optical dating of single and multiple grains of quartz from Jinmium rock shelter, northern Australia: part I, experimental design and statistical models. *Archaeometry* **41**, 339–364.

Galli, A., Panzeri, L., Rondini, P., Poggiani Keller, R., Martini, M., 2020. Luminescence dating of rock surface. The case of monoliths from the megalithic sanctuary of Ossimo-Pat (Valle Camonica, Italy). *Applied Sciences* **10**, 7403.

García Sanjuán, L., Aranda Jiménez, G., Carrión Méndez, F., Mora Molina, C., Lozano Medina, Á., García González, D., 2016. El relleno del pozo de

https://doi.org/10.1017/qua.2022.33 Published online by Cambridge University Press

Menga: estratigrafía y radiocarbono. *Menga: Revista de Prehistoria de Andalucía* **7**, 199–223.

García Sanjuán, L., Fernández Rodríguez, L. E., Balsera Nieto, V., Mora Molina, M., Lozano Rodríguez, J.A., Cisneros García, M., López Sáez, J.A., *et al.*, 2020. Builders of megaliths: society, monumentality and environment in 4th millennium cal BC Antequera. *Journal of Archaeological Science: Reports* **33**, 102555.

García Sanjuán, L., Lozano Rodríguez, J.A., 2016. Menga (Andalusia, Spain): biography of an exceptional megalithic monument, In: Laporte, L., Scarre, C. (Eds.), *The Megalithic Architectures of Europe*. Oxbow, Oxford, pp. 3–16.

García Sanjuán, L., Montero Artús, R., Mora Molina, C., 2021. Waterscapes through time: the Menga well as a unique hydraulic resource in its geographic and historical context. In: Bartelheim, M., García Sanjuán, L., Hardenberg, R. (Eds.), *Human-Made Environments: The Development of Landscapes as Resource Assemblages*. RessourcenKulturen 15. Tübingen University Press, Tübingen, pp. 89–116.

García Sanjuán, L., Mora Molina, C., Lozano Medina, Á., Aranda Jiménez, G., 2018a. La cronología radiocarbónica del dolmen de Menga. In: García Sanjuán, L., Mora Molina, C. (Eds.), *La Intervención de 2005 en el Dolmen de Menga. Temporalidad, Biografía y Cultura Material en un Monumento del Patrimonio Mundial, Sevilla*. Junta de Andalucía y Universidad de Sevilla, Seville, pp. 307–322.

García Sanjuán, L., Sánchez Díaz, F., Morell Rovira, L., 2022. The "Megalithisation" of Iberia: a spatio-temporal model. *L' Anthropologie* (in press).

García Sanjuán, L., Vargas Jiménez, J.M., Cáceres Puro, L., Costa Caramé, M.E., Díaz-Guardamino-Uribe, M., Díaz-Zorita Bonilla, M., Fernández Flores, Á., *et al.*, 2018b. Assembling the dead, gathering the living: radiocarbon dating and Bayesian modelling for Copper Age Valencina de la Concepción (Sevilla, Spain). *Journal of World Prehistory* **31**, 179–313.

García Sanjuán, L., Wheatley, D.W., Díaz-Guardamino Uribe, M., Mora Molina, C., Sánchez Liranzo, O., Strutt, K., 2015. Evidence of Neolithic activity at La Peña de los Enamorados (Antequera, Málaga): intensive surface survey, geophysics and geoarchaeology at the site of Piedras Blancas I, *Menga. Revista de Prehistoria de Andalucía* **6**, 211–252.

Garnier, N., García Sanjuán, L., Dodinet, E., Cintas-Peña, M., Guilaine, J., 2022. Las cerámicas neolíticas del túmulo del dolmen de Menga: análisis de contenidos. In: García Sanjuán, L. (Ed.), *La Intervención de 2005–2006 en el Dolmen de Menga: Investigando la Génesis de Un Monumento Neolítico Excepcional*. Universidad de Sevilla and Editorial Almuzara, Seville.

Grützner, C., Ruano, P., Jabaloy, A., Galindo-Zaldívar, J., Becker-Heidmann, P., Sanz De Galdeano, C., Rudersdorf, A., Reicherter, K., 2013. Late Holocene rupture history of the Ventas de Zafarraya Fault (southern Spain). *Cuaternario y Geomorfología* **27**, 51–61.

Guilaine, J., 2011. Megaliths in France: geographic distribution and chronology. In: García Sanjuán, L., Scarre, C., Wheatley, D. (Eds.), *Exploring Time and Matter in Prehistoric Monuments: Absolute Chronology and Rare Rocks in European Megaliths. Proceedings of the 2nd EMSG Meeting (Seville, November 2008)*. Junta de Andalucía, Seville, pp. 77–101.

Hoffmann, D.L., Pike, A.W.G., García-Díez, M., Pettitt, P.B., Zilhão, J., 2016. Methods for U-series dating of $CaCO_3$ crusts associated with Palaeolithic cave art and application to Iberian sites. *Quaternary Geochronology* **36**, 104–119.

Hoffmann, D.L., Prytulak, J., Richards, D.A., Elliott, T., Coath, C.D., Smart, P.L., Scholz, D., 2007. Procedures for accurate U and Th isotope measurements by high precision MC-ICPMS. *International Journal of Mass Spectrometry* **264**, 97–109.

Hoffmann, D.L., Standish, C.D., García-Diez, M., Pettitt, P.B., Milton, J.A., Zilhão, J., Alcolea-González, J.J., *et al.*, 2018. U-Th dating of carbonate crusts reveals Neandertal origin of Iberian cave art. *Science* **359**, 912–915.

Hoskin, M., 2001. *Tombs, Temples and Their Orientation. A New Perspective on Mediterranean Prehistory*. Ocarina, Oxford.

Jaffey, A.H., Flynn, K.F., Glendenin, L.E., Bentley, W.C., Essling, A.M., 1971. Precision measurement of half-lives and specific activities of U235 and U238. *Physical Review C* **4**, 1889.

Kagan, E. J., Agnon, A., Bar-Matthews, M., Ayalon, A., 2005. Dating large infrequent earthquakes by damaged cave deposits. *Geology* **33**, 261–264.

Kim, S.J., Choi, J.H., Lim, H.S., Shin, S., Yeo, E.Y., Weon, H.J., Heo, S., 2022. Multiple and single grain quartz OSL dating of dolmens in Jungdo, central Korean Peninsula. *Geosciences Journal*. https://doi.org/10.1007/s12303-022-0002-5.

Laporte, L., Cousseau, F. (Eds.), 2020. *Pre and Protohistoric Stone Architectures: Comparisons of the Social and Technical Contexts Associated to their Building. Proceedings of the XVIII UISPP World Congress (4–9 June, Paris, France)*. Archaeopress, Oxford.

Lario, J., Zazo, C., Goy, J.L., Silva, P.G., Bardají, T., Cabero, A., Dabrio, C.J., 2010. Registro geológico de tsunamis en el SW peninsular durante el Holoceno. In: Insua Arévalo J.M., Martín González, F. (Eds.), *Contribución de la geología al análisis de la peligrosidad sísmica. Primera reunión Ibérica sobre fallas activas y paleosismología*. Libro de resúmenes. Iberfault, Sigüenza, Spain, pp. 167–170.

Lindley, D.V., 1985. *Making Decisions*. Wiley, London.

Liritzis, I., 2011. Surface dating by luminescence: an overview. *Geochronometria* **38**, 292–302.

López Romero, E., 2011. OSL dating of megalithic monuments: context and perspectives, In: García Sanjuán, L., Scarre, C., Wheatley, D. (Eds.), *Exploring Time and Matter in Prehistoric Monuments: Absolute Chronology and Rare Rocks in European Megaliths. Proceedings of the 2nd EMSG Meeting (Seville, November 2008)*. Junta de Andalucía, Seville, pp. 193–214.

Lozano Rodríguez, J.A., García Sanjuán, L., Mora Molina, C., Masclans Latorre, A., Martínez-Sevilla, F., Gibaja Bao, J.F., 2018a. El material macrolítico del dolmen de Menga. In: García Sanjuán, L., Mora Molina, C. (Eds.), *La intervención de 2005 en el dolmen de Menga: temporalidad, biografía y cultura material en un monumento del Patrimonio Mundial*. Junta de Andalucía, Seville, pp. 207–238.

Lozano Rodríguez, J.A., Martínez-Sevilla, F., Sánchez Liranzo, O., Gibaja Bao, J.F., Masclans Latorre, A., Mora Molina, C. y García Sanjuán, L., 2018b. El material lítico tallado del dolmen de Menga: caracterización tecno-morfológica y litológica y análisis traceológico. In: García Sanjuán, L., Mora Molina, C. (Eds.), *La intervención de 2005 en el dolmen de Menga: temporalidad, biografía y cultura material en un monumento del Patrimonio Mundial*. Junta de Andalucía, Seville, pp. 189–206.

Lozano Rodríguez, J.A., Morgado Rodríguez, A., 2012. La explotación prehistórica de afloramientos de rocas ofíticas del sector oriental del "Trías de Antequera" (España). In: Peinado Herreros, A. (Ed.), *El patrimonio cultural y natural como motor de desarrollo: investigación e innovación*. Universidad Internacional de Andalucía, Jaén, pp. 1503–1517.

Lozano Rodríguez, J.A., Morgado Rodríguez, A., Puga Rodríguez, E., Martín Algarra, A., 2010. Explotaciones del sílex tipo Turón (Málaga, España): localización y caracterización petrológica y geoquímica. *Geogaceta. Sociedad Geológica de España* **48**, 163–166.

Lozano Rodríguez, J.A., Ruiz Puertas, G., Hódar Correa, M., Pérez Valera, F., Morgado Rodríguez, A., 2014. Prehistoric engineering and astronomy of the great Menga dolmen (Málaga, Spain). A geometric and geoarchaeological analysis. *Journal of Archaeological Science* **41**, 759–771.

Marques, R., Prudêncio, M.I., Russo, D., Cardoso, G., Dias, M.I., Rodrigues, A.L., Reis, M., Santos, M., Rocha, F., 2021. Evaluation of naturally occurring radionuclides (K, Th and U) in volcanic soils from Fogo Island, Cape Verde. *Journal of Radioanalytical and Nuclear Chemistry* **330**, 347–355.

Martínez Torres, L.M., 2015. *Aspectos Geóticos de los Menhires Alaveses*. Diputación Foral de Álava, Vitoria, Spain.

Martín Socas, D., Cámalich Massieu, M.D., González Quintero, P. (Eds.), 2004. *La Cueva del Toro (Sierra del Torcal, Antequera, Málaga). Un Modelo de Ocupación Ganadera en el Territorio Andaluz Entre el VI y II Milenios ANE*. Junta de Andalucía, Seville.

Medialdea, A., Thomsen, K.J., Murray, A.S., Benito, G., 2014. Reliability of equivalent-dose determination and age-models in the OSL dating of historical and modern palaeoflood sediments. *Quaternary Geochronology* **22**, 11–24.

Meller, H., Gronenborg, D., Risch, R. (Eds.) 2018. *Surplus Without the State: Political Forms in Prehistory (10th Archaeological Conference of Central Germany, Halle, October 19–21 2018)*. Landesmuseum für Vorgeschichte, Halle, Germany.

Mitjana y Ardison, R. 1847. *Memoria sobre el Templo Druida Hallado en las Cercanías de la Ciudad de Antequera*. Imprenta de D. José Martínez Aguilar, Málaga.

https://doi.org/10.1017/qua.2022.33 Published online by Cambridge University Press

Mora Molina, C., 2018. *Los Monumentos Megalíticos de Antequera: Una Aproximación Biográfica*. Unpublished PhD thesis. Universidad de Sevilla, Seville.

Morgado Rodríguez, A., García-Alfonso, E., García del Moral, L.F., Benavides, J.A., Rodríguez-Tovar, F.J., Esquivel, J.A., 2018. Embarcaciones prehistóricas y representaciones rupestres. Nuevos datos del abrigo de Laja Alta (Jimena de la Frontera, Cádiz). *Complutum* **29**, 239–265.

Morgado Rodríguez, A., Lozano Rodríguez, J.A., 2011. The impact of geological factors on flint mining and large blade production in the Betic Cordillera (Spain, Mill IV–III BC). In: *Proceedings of the 2nd International Conference of the UISPP Commission on Flint Mining in Pre- and Protohistoric Times*. BAR International Series 2260. Archaeopress, Oxford, pp. 183–191.

Morgado Rodríguez, A., Lozano Rodríguez, J.A., 2012. Objetos de sílex, marcadores litológicos de la circulación. In: García Alfonso, E. (Ed.), *Geoarqueología de la producción laminar especializada del sur de Iberia (c. VI-V mil. cal. BP). Movilidad, Contacto y Cambio. Actas del II Congreso de Prehistoria de Andalucía (Antequera, Málaga, 15, 16 y 17 de febrero de 2012)*. Junta de Andalucía, Seville, pp. 121–136.

Morgado Rodríguez, A., Martínez Sevilla, F., Lozano Rodríguez, J.A., 2013. Tallar para pulir. Experimentación sobre la elaboración de hachas pulimentadas de rocas ofíticas en el sur de la Península Ibérica. In: Palomo, A., Piqué, R., Terrada, X. (Eds.), *Experimentación en Arqueología. Estudio y difusión del pasado. Experimentación en Arqueología*. Museu Arqueologia de Catalunya, Barcelona, pp. 107–116.

Müller, J., Hinz, M., Wunderlich, M. (Eds.) 2019. *Megaliths, Societies, Landscapes. Early Monumentality and Social Differentiation in Neolithic Europe*. Frühe Monumentalität und soziale Differenzierung 18. Kiel University, Kiel, Germany.

Murray, A.S., Wintle, A.G., 2000. Luminescence dating of quartz using an improved single-aliquot regenerative-dose protocol. *Radiation Measurements* **32**, 57–73.

Odriozola Lloret, C., Burbidge, C.I., Isabel Días, M., Hurtado, V., 2014. Dating of las mesas Copper Age walled enclosure (La Fuente, Spain)/ Datación del recinto murado calcolítico de Las Mesas (La Fuente, España). *Trabajos de Prehistoria* **71**, 343–352.

Parker Pearson, M., 2012. *Stonehenge: Exploring the Greatest Stone Age Mystery*. Simon and Schuster, London.

Parker Pearson, M., Pollard, J., Richards, C., Welham, K., Kinnaird, T., Shaw, D., Simmons, E., *et al.*, 2021. The original Stonehenge? A dismantled stone circle in the Preseli Hills of west Wales. *Antiquity* **95**, 85–103.

Patrick, J., 1974. Midwinter sunrise at Newgrange. *Nature* **249**, 517–519.

Peñalver Iribarren, X., 1989. Estudio de los menhires de Euskal Herría. *Munibe* **35**, 355–450.

Peñalver Iribarren, X., 2011. *Dólmenes, Cromlech y Menhires. Guía Básica del Megalitismo en Euskal Herría*. Txertoa, San Sebastián, Spain.

Querré, G., Calligaro, T., Cassen, S., 2019. Origine des bijoux néolithiques en Callaïs de l'ouest de la France. In: Querré, G., Cassen, S., Vigier E. (Eds.), *La Parure en Callaïs du Néolithique Européen*. Archaeopress, Oxford, pp. 129–198.

Reimer, P.J., Austin, W.E., Bard, E., Bayliss, A., Blackwell, P.G., Bronk Ramsey, C., Burtzin *et al.*, 2020. The IntCal20 Northern Hemisphere radiocarbon age calibration curve (0–55 cal kBP). *Radiocarbon,* **62**, 725–757.

Renfrew, C., 1973. Monuments, mobilisation and social organisation in Neolithic Wessex. In: Renfrew, C. (Ed.), *The Explanation of Culture Change. Models in Prehistory*. Duckworth, London, pp. 539–558.

Richter, D., Zink, A.J.C., Przegietka, K.R., Cardoso, G.O., Gouveia, M.A., Prudêncio, M.I., 2003. Source calibrations and blind test results from the new Luminescence Dating Laboratory at the Instituto Tecnológico e Nuclear, Sacavém, Portugal. *Ancient TL* **21**, 43–48.

Rivollat, M., Choongwon, J., Schiffels, S., Küçükkalipçi, I., Pemonge, M.H., Rohrlach, A.B., Alt, K.W., *et al.*, 2020. Ancient genome-wide DNA from France highlights the complexity of interactions between Mesolithic hunter-gatherers and Neolithic farmers. *Science Advances* **6**, 1–16.

Rodrigues, A.L., Dias, M.I., Valera, A.C., Rocha, F., Prudêncio, M.I., Marques, R., Cardoso, G., Russo, D., 2019. Geochemistry, luminescence and innovative dose rate determination of a Chalcolithic calcite-rich negative feature. *Journal of Archaeological Science: Reports* **26**, 101887.

Rogerio-Candelera, M.Á., Bueno Ramírez, P., De Balbín Behrmann, R., Dias, M.I., García Sanjuán, L., Coutinho, M.L., Lozano Rodríguez, J.A., *et al.*, 2018. Landmark of the past in the Antequera megalithic landscape: a multi-disciplinary approach to the Matacabras rock art shelter. *Journal of Archaeological Science* **95**, 76–93.

Sánchez-Cuenca, J.I., 2011. *Menga en el Siglo XIX. El Más Bello y Perfecto de los Dólmenes Conocidos*. Menga: Revista de Prehistoria de Andalucía, Monografías 2. Junta de Andalucía, Seville.

Santana, J., Rodríguez-Santos, F.J., Cámalich-Massieu, M.D., Martín-Socas, D., Fregel, R., 2019. Aggressive or funerary cannibalism? Skull-cup and human bone manipulation in Cueva de El Toro (Early Neolithic, southern Iberia). *American Journal of Physical Anthropology* **169**, 1–24.

Santos Arévalo, F.J., Gómez Martínez, I., García León, M., 2009. Radiocarbon measurement program at the Centro Nacional de Aceleradores (CNA), Spain. *Radiocarbon* **51**, 883–889.

Schulz Paulsson, B., 2019. Radiocarbon dates and Bayesian modelling support maritime diffusion model for megaliths in Europe. *Proceedings of the National Academy of Sciences USA* **116**, 3460–3465.

Sherratt, A., 1990. The genesis of megaliths: monumentality, ethnicity and social complexity in Neolithic north-west Europe. *World Archaeology* **22**, 147–167.

Shewan, L., O'Reilly, D., Armstrong, R., Toms, P., Webb, J., Beavan, N., Luangkhoth, T., *et al.*, 2021. Dating the megalithic culture of Laos: radiocarbon, optically stimulated luminescence and U/Pb zircon results. *PLoS ONE* **16**, e0247167.

Thomsen, K.J., Murray, A.S., Bøtter-Jensen, L., Kinahan, J., 2007. Determination of burial dose in incompletely bleached fluvial samples using single grains of quartz. *Radiation Measurements* **42**, 370–379.

Wedepohl, K.H., 1995. The composition of the continental crust. *Geochimica et Cosmochimica Acta* **59**, 1217–1232.

Whittle, A., 2018. *Times of Their Lives. Hunting History in the Archaeology of Neolithic Europe*. Oxbow, Oxford.

https://doi.org/10.1017/qua.2022.33 Published online by Cambridge University Press